Assessing relative biomarker responses in marine and freshwater bivalve molluscs following exposure to phosphorus 32 (^{32}P): Application of genotoxicological and molecular biomarkers

Abstract

Anthropogenic radionuclides can enter water bodies through accidental or controlled discharges. In order to assess their potential impact, understanding the link between exposure, tissue specific bioaccumulation and radiation dose rate, to biological or biomarker responses in aquatic biota is required. Adopting an integrated, multi-biomarker, multi-species approach, we have investigated potential biological responses induced by short-lived radionuclide, phosphorus-32 (^{32}P, radiophosphorus) in two ecologically important mussel species, the freshwater *Dreissena polymorpha* (DP) and marine *Mytilus galloprovincialis* (MG). Adult individuals were exposed to ^{32}P for 10 days, to acquire nominal whole-body average dose rates of 0.10, 1 and 10 mGy d^{-1}, which encompass a screening value of 10 µGy h^{-1} (0.24 mGy d^{-1}), in accordance with the ERICA tool. Following exposure, a suite of genotoxic biomarkers (DNA damage, γ-H2AX induction and micronucleus [MN] formation) were measured in gill and digestive gland tissues, along with transcriptional expression of selected stress-related genes in both the species (i.e. *hsp70/90, sod, cat and gst*). Our results demonstrate the relationship between tissue specific dosimetry, where ^{32}P induced a dose-dependent increase, and biological responses independent of species. Gene expression analysis revealed little significant variation across species or tissues. Overall, MG appeared to be more sensitive to short-term damage (i.e. high DNA damage and γ-H2AX induction), particularly in digestive gland. This study contributes to limited knowledge on the transfer and biological impact of radionuclides within differing aquatic systems on a tissue specific level, aiding the development of adequate management and protective strategies.

Keywords: Bivalves, ^{32}Phosphorus, ionising radiation, genotoxicity, gene expression, γ-H2AX

Abbreviations: µg, Microgram; µM, Micromole; γ-H2AX, Gamma-H2AX; ^{32}P, Phosphorus 32; ATP, Adenosine triphosphate; CAT, Catalase; Cu, Copper; DAPI, 4′,6-diamidino-2-phenylindole dihydrochloride; DDR, DNA damage response; DO, Dissolved oxygen; DP, *Dreissena polymorpha*; DSB, Double strand break; ERICA, Environmental Risk from Ionising Contaminants Assessment & Management Tool; GST, Glutathione-S-Transferase; HCl, Hydrochloric acid; HSP, Heat Shock Protein; ICP-MS, Inductively coupled plasma mass spectrometry; LET, Linear energy transfer; LSC, Liquid scintillation counter; IR, Ionising radiation; MG, *Mytilus galloprovincialis*; MN, Micronuclei; MOA, Mode of action; RER, Relative mRNA expression ratio; ROS, Reactive oxygen species; SOD, Superoxide Dismutase; SSB, Single strand break.

1. Introduction

Radionuclides discharged in the environment can pose short and long-term detrimental effects to both human and natural biota (UNSCEAR, 1982; Dallas et al., 2012). With rapid population growth driving the need for nuclear energy, along with accidental (e.g. Chernobyl, 1986; Fukushima, 2011) and controlled release (i.e. from educational, medical and other establishments), radionuclides are of concern to both scientific and regulatory bodies (Hu et al., 2010; Khamis and Kavvadias, 2012). While there is not enough experimental information available in the literature to develop a screening dose rate for each species (Dallas et al., 2012), a dose rate of 10 μGy h^{-1} (0.24 mGy d^{-1}) has been adopted as a generic screening value (all species), where no significant negative effects are expected at the population level (Andersson et al., 2008, 2009). Where this value will over protect some biota and under protect others, it can be used as a benchmark to screen out situations of no regulatory concern. As explained in previous literature (Vernon et al., 2018), a whole-body dose monitoring approach may be insufficient in wholly protecting organisms from radiation exposure, as radionuclides are known to display specificity in tissue uptake. As such, a specific tissue (e.g. digestive gland) accumulating a significant proportion of a radionuclide, compared to another tissue would receive a far higher dose and therefore, a higher degree of biological damage. Whole-body monitoring may therefore mask tissue specific damage. To ensure an adequate degree of protection, impacts at sub-organismal and individual levels need to be extrapolated and related to those at the population, community, or ecosystem level. Linking radiation exposure to tissue specific bioaccumulation and dose rate, and to subsequent biological responses in a range of aquatic organisms to establish relative radiation sensitivities will aid this

extrapolation (Scoppa, 1983; Dallas et al., 2012; Kumar et al., 2017; Carvalho, 2018; Salbu et al., 2018; Skipperud and Salbu, 2018; Vernon et al., 2018).

To date, the majority of radiation studies have focused primarily on external exposures to long-lived radionuclides, where whole-body dose rates are related to biological response. However, short-lived radionuclides such as ^{32}P (half-life = 14.29 d), whilst occurring in small quantities within the environment have the capacity to accumulate in aquatic biota, particularly when they are chronically exposed (Smith et al., 2011). When accumulated, internal exposure within cells/tissue can induce significant biological damage dependant on the radionuclide and typical range in tissue (e.g. alpha particles have short range in tissue, ~0.3 mm) (Cherry et al., 2012).

Environmental ^{32}P originates from various sources (e.g. cosmogenic and anthropogenic) but there is paucity of information about its presence in the environment. While the half-life of this radionuclide is short, it is discharged and detected in the aquatic environment. In terms of recorded environmental concentrations, ^{32}P values (2005-2013) average 0.27 ± 0.21 Bq L^{-1} in the River Clyde (Erskine Habour, King George V Dock), Scotland (SEPA, 2013). Reference conditions for ^{32}P (i.e. concentrations that result in a total ingested dose for humans of 0.10 mSv y^{-1} if consumed at 2 L day^{-1}), are set at 57 Bq L^{-1} (DWQR, 2014). While not as environmentally prominent as other radionuclides such as caesium-137 (^{137}Cs), cobalt-60 (^{60}Co), and tritium (^{3}H), ^{32}P can be utilised as a relatively cheap, easy to use (in terms of experimental design) surrogate for beta and gamma emitting radionuclides (Vernon et al., 2018), capable of producing an internal and external exposure to study biological responses in appropriate models. Furthermore, whilst appearing in small concentrations within the environment as mentioned above, ^{32}P is able to rapidly accumulate to high concentrations in tissues and could induce detrimental effects in a

tissue specific manner (Vernon et al., 2018). Our recent study has reported highly tissue specific accumulation in marine and freshwater bivalves, where the greatest ^{32}P concentrations were present in the digestive gland (Vernon et al., 2018). Once concentrated in tissues, the radioisotope has the potential to cause significant molecular and genetic level effects. ^{32}P is chemically and radiologically unique as the mode of actions (MoA) is mediated by DNA double-strand break (DSB) induction (Cheng et al., 2015). Aqueous ^{32}P gets incorporated into the ribose-phosphate backbone of replicating DNA, isotopic decay (^{32}P to sulfur-32, ^{32}S) results in chemical breakage of DNA (SSBs), and the release of high energy beta particles causes further DNA damage through double strand breaks (DSBs) (Cheng et al., 2015). It should be noted that the term 'DNA damage' will refer to strand breakage as measured by the comet assay whereas DNA damage/ repair response will be referred as Gamma-H2AX assay in this study.

Ionising radiations (IR) primarily influence sub-cellular levels of biological organisation by interacting with atoms of biomolecules (Bayliss and Langley, 2003). Therefore, molecular and genetic alterations are perceived as an early warning signal of organism's stress (Bayliss and Langley, 2003; Czapla-Masztafiak et al., 2016). Due to (a) the radiological nature of ^{32}P, (b) its accumulative potential in aquatic biota and (c) the limited amount of information available with respect to possible impacts of short-lived radionuclides on the biota, we aimed to investigate potential genetic and molecular alterations in two bivalve species, inhabiting different environments. Measured biological responses included DNA damage and repair, micronuclei (MN) formation, and changes in the transcription of key genes involved in stress responses, given that the earliest observable signs of biological stress can be transcriptional alteration of the genes (Bahrami and Drabløs, 2016). To date, there is limited

information available on IR induced mRNA alterations in aquatic invertebrates (Gomes et al., 2018; Han et al., 2014a, b; Farcy et al., 2007, 2011; AlAmri et al., 2012; Devos et al., 2015; Dallas et al., 2016). More studies are required, particularly as most of the information available in the literature have evaluated expression of genes and other biological responses following exposure of organisms to acute, external radiation sources (i.e. ^{137}Cs), which could not be considered as environmentally relevant as chronic, low-dose exposures (Dallas et al., 2012).

In the present study, we investigated ^{32}P-induced potential biological damage in two ecologically important bivalve species, the marine mussel *Mytilus galloprovincialis* (MG), and freshwater species *Dreissena polymorpha* (DP). Bivalve molluscs utilised in the study represent both coastal and inland water bodies (McDonald et al., 1991; Binelli et al., 2015). Where marine species might not be used to determine risk in freshwater environments or vice-versa, it is important to determine biological damage associated with radionuclide exposure in the biota belonging to the same biological group. This would assist in identifying the most sensitive species for environmental protection (Vernon and Jha, 2019), and will add to the paucity of radioecological/radiotoxicity data, particular for freshwater bivalves (Falfushynska et al., 2016; Vernon et al., 2018). As sessile, filter feeders, bivalves play an important role as bioindicators of environmental health (Hawkins, 1992; Viarengo et al., 2007; NOAA, 2012; Souza et al., 2012). Their prominent use in ecotoxicological studies has resulted in a well-understood physiology, anatomy and ecology (Bayne, 1976; Dallas et al., 2012; Binelli et al., 2015; Beyer et al., 2017; Vernon et al., 2018). Digestive gland and gill tissues were utilised as in previous studies from our laboratory. This allowed for comparison between biological responses in tissues exhibiting varying accumulation patterns. As noted in Vernon et al. (2018), ^{32}P accumulation, and

therefore dose rate is far greater in digestive gland compared to other soft tissues (i.e. gill, mantle). Mussel digestive glands accumulate and process nutrients, which are distributed to reproductive tissues during gonad development. As such, apart from impact on overall homeostatic control, the key concern with digestive gland damage is the possible influence on reproductive success (Sastry and Blake, 1971; Dimitriadis et al., 2004). Mussel gills play a major role in respiratory processes, nutrient uptake and digestion (David and Fontanetti, 2005; Gómez-Mendikute et al., 2005). They filter suspended particulates directly from the surrounding media to specific organs (Jørgensen, 1982). The large surface area and close proximity to aquatic contaminants makes them a prime tissue for biomonitoring and ecotoxicological studies and their sensitivity to numerous pollutants is well documented (Mersch et al., 1996; Parolini et al., 2011; Al-Subiai et al., 2012; Canesi et al., 2014; Dallas et al., 2013, 2016, 2018).

The aims and objectives of this study were: (a) to relate radionuclide (i.e. ^{32}P) bioaccumulation and delivered dose rate to subsequent biological responses, in gill and digestive gland tissues of the selected bivalves, (b) to determine genotoxic and molecular responses in two bivalves following ^{32}P exposure adopting a multi-biomarker approach and (c) to determine relative sensitivity between marine and freshwater adult bivalves. We hypothesised that as ^{32}P uptake, and therefore dose rate increases, as will the level of biological damage. In terms of variation between bivalve species subsequent to ^{32}P exposure, we hypothesised that little disparity in genotoxic or molecular response would be evident, increased DNA damage would be paralleled by DDR, and lastly, genes related to oxidative stress would be upregulated following ^{32}P exposure.

2 Materials and methods

2.1.1 Chemicals and suppliers

Commercially available, radiolabelled-ATP (Adenosine triphosphate, γ-32P), was obtained from Perkin Elmer (PerkinElmer, UK) in batches of 9.25 MBq (specific activity concentration: 370 MBq mL^{-1}), and diluted with DI water to form appropriate working solutions. Radiolabelled ATP was utilised in our experiments as (a) the ATP itself would not cause biological damage due to chemical similarities between radio and stable isotope and (b) it would not affect the chemical composition (i.e. salinity, pH) of the salt/freshwater (Vernon et al., 2018). Working solution added to exposure beakers was decay adjusted. All chemicals and reagents were purchased from Perkin Elmer (PerkinElmer, UK), Lab Logic (LabLogic systems Ltd., UK), Fisher Scientific UK, Anachem Ltd., UK, Sigma-Aldrich Company Ltd., UK, VWR International Ltd., USA or Greiner Bio-One Ltd. UK, unless stated otherwise. Product details are noted in text as appropriate.

2.1.2 Mussel exposure conditions

Two ten-day sequential exposure experiments were performed in June and September 2017 (Fig. 1). Mussels were collected and maintained in the same way as other studies from our laboratory (Dallas et al., 2013, 2016; Pearson et al., 2018; Vernon et al., 2018). *Mytilus* sp. designation was confirmed prior to exposure as described before (Pearson et al., 2018; Vernon et al., 2018). In brief, MG were maintained in UV treated, filtered (< 10 µm), aerated, natural seawater (MG) and fed a solution of *Isochrysis galbana* algae ($8x10^5$ cells/mL, Reed Mariculture, Campbell, CA, USA). DP mussels were maintained in UV treated, filtered (< 10 µm), aerated artificial river water solution and fed dried *Chlorella* powder (3.2 mg/mussel, Naturya, Bath, UK). Both species were maintained at a 12:12 h photoperiod at 15 °C.

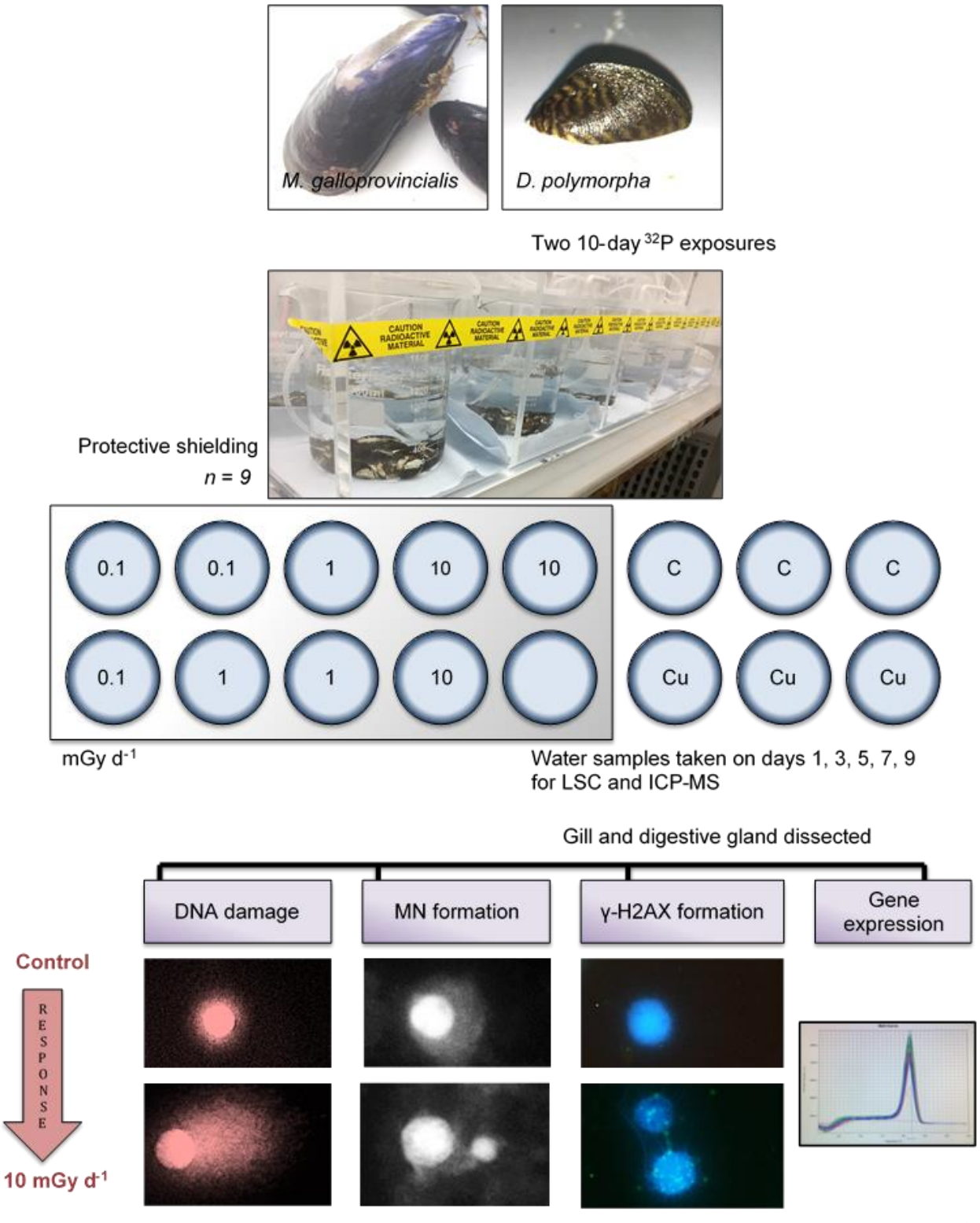

Figure 1. Schematic diagram showing experimental design. Images from *M. galloprovincialis* digestive gland cells.

Exposures were staggered by one week for ease of analysis and logistical reasons. MG (shell length 45.2 ± 4.6 mm) and DP (shell length 25.9 ± 3.2 mm) individuals (total weight, 35 g L^{-1}) per labelled beaker were exposed to the following activity concentrations of ATP [γ-32P] in triplicate: 993, 9930, 99300 and 289, 2892, 28928 Bq L^{-1}, respectively, to meet the expected dose rates of 0.10, 1.00 and 10 mGy d^{-1}. Nominal ^{32}P activity levels in water were calculated from preliminary experiments (data not included; (Vernon et al., 2018). A negative control and positive control (copper [Cu], as CuSO4.5H2O, 99% purity, 56 µg L^{-1}) were run alongside to compare the biological responses. Concentration of Cu used as positive control was selected in accordance to previous work from our laboratory and in line with environmentally realistic values (Al-Subiai et al., 2011; D'Agata et al., 2014). Water changes (50 %) were carried out on days 3, 5, 7 and 9. ^{32}P activity levels were determined via water samples (1 mL, in duplicate), taken ~30 min after each water change and processed for liquid scintillation counting (LSC) as in section 2.3.1. Mussels were fed 2 h prior to water changes as described in earlier studies (Vernon et al., 2018). As DP are an invasive species in the UK (Nalepa and Schloesser, 1992; Karatayev et al., 2007), waste freshwater was spiked with salt (50 g L^{-1}, NaCl) before disposal as to prevent infestation and dispersal. All radioactive wastewater (salt and fresh) was stored for 4 months (~ 8 half-lives) before disposal to allow for decay. Water quality parameters were measured routinely, before and after water changes. ^{32}P and Cu concentrations were determined as per standard procedures (described below in section 2.3), along with water quality measurements, which are displayed in Table 1. Data from LSC counting and ICP-MS analysis confirmed that achieved values were in line with expected concentrations across all treatments.

Table 1. Water quality parameters (pH, temperature, salinity and dissolved oxygen [DO]), copper concentrations in water (µg L^{-1}) and ^{32}P concentrations in water (Bq L^{-1}), for both species. Data is presented as mean ± standard deviation.

Water parameters	***M. galloprovincialis***	***D. polymorpha***
pH	8.1 ± 0.96	8.2 ± 0.18
Temp (°C)	14.8 ± 0.16	14.8 ± 0.16
Salinity	33.7 ± 0.34	0.3 ± 0.01
DO (%)	99.7 ± 1.14	100.5 ± 0.85
Copper water conc. (µg L^{-1})		
Control	0.1 ± 0	0.1 ± 1
56	43.5 ± 8.52	59.7 ± 3.74
^{32}P water conc. (Bq L^{-1})		
Control	0.2 ± 0.60	0.3 ± 0.44
993 / 289	1032.2 ± 327.63	263.9 ± 95.85
9930 / 2892	9916.1 ± 1120.82	2687 ± 395.37
99300 / 28928	98716.7 ± 6429.27	26561 ± 2776.52

2.1.3 Sampling procedures

Subsequent to exposures, gill and digestive gland tissues were dissected from each individual as described in detail in earlier studies from our laboratory (Dallas et al., 2013; Pearson et al., 2018; Vernon et al., 2018). Dissected tissues were stored as followed until use: $^{2}/_{3}$ tissue stored in tube on ice until cell isolation, $^{1}/_{3}$ stored in RNAlater (1.5 mL, Fisher UK) at -20 ºC. All other soft tissues and shell were discarded following a 4 month storage period, allowing for decay.

2.2 Biological assays

2.2.1 Isolation of digestive gland and gill cells

The procedure to obtain gill and digestive gland cells was adapted from earlier studies (Vincent-Hubert et al., 2011), with minor adjustments. 1 mL dispase II solution (1.6 mg dispase powder per 1 mL of HBSS, Sigma) was added per sample. Samples were incubated for 30 min (37 ºC); shaken every 10 min. Following incubation, cell suspension was centrifuged (775 g, 5 min). Supernatant was utilised in subsequent assays, cell viability was <90% across all treatments, as checked using the Trypan Blue exclusion dye assay (Strober, 2001), data not Included). To avoid bias, all assays were scored blind.

2.2.2 Comet assay to determine DNA strand breaks

Determination of DNA strand breakage using the single-cell gel-electrophoresis, or comet assay was performed as described in detail in earlier publications (Jha et al., 2005; Cheung et al., 2006; Al-Subiai et al., 2011; Dallas et al., 2013; Pearson et al., 2018) with minor modifications. Prior to *in vivo* studies, the assay was validated under *in vitro* and *in vivo* conditions using a range of concentrations of hydrogen peroxide (1 h exposure) and copper (10 d exposure) (unpublished results; Dallas et al., 2013; Vernon and Jha, 2019). Gill and digestive gland cell suspensions (see section 2.2.1, 150 µL) were used immediately for the assay. A cell-agarose suspension (1% LMA, Sigma-Aldrich Company Ltd UK) was pipetted in duplicate onto a pre-coated (1% NMA in TAE) slide and left to set (4 °C, ~1 h). Slides were then placed in a chilled lysis buffer (1 h, 4 ºC) and denatured in an electrophoresis buffer (20 min, 0.3 M NaOH and 1 mM EDTA, at pH 13). Electrophoresis was run for 25 min at 21 V and 620 mA. Slides were placed in a neutralisation buffer (0.4 M Tris Base, Sigma) for 5 min and then into

chilled distilled water for 5 min. Ethidium bromide (20 µL of 20,000 µg L^{-1}) was used to stain nuclei; slides were scored using an epifluorescent microscope (DMR; Leica Microsystems, Milton Keynes, UK). 100 cells per coded slide were scored using the Comet IV imaging software (Perceptive Imaging, Bury St Edmunds, UK). The software provides results for different parameters, % Tail DNA was considered the most reliable to present the results (Kumaravel and Jha, 2006).

2.2.3 Analysis of micronuclei (MN) induction

Cell suspension (see section 2.2.1, 50 µL) was allowed to adhere onto a coded slide for 1 h at 4 ºC) prior to fixation. To fix, ice-cold Carnoys solution was gently pipetted onto each slide (1 mL, 20 min, 75% methanol, 25% glacial acetic acid). Fixative was removed and slides were rinsed gently with DI water. To score, slides were stained with ethidium bromide as in section 2.2.2. 500 cells were scored per coded slide at random, using a fluorescent microscope (as in section 2.2.2). MN were identified in accordance to Venier et al. (1997) and Bolognesi and Fenech. (2012). Results are reported as mean MN per 1000 cells in accordance with other data published from our laboratory (Dallas et al., 2013).

2.2.4 Induction of γ-H2AX foci

Due to its highly conserved nature between species (Foster and Downs, 2005; Liu et al., 2011), we were able to utilise antibodies from differing species to measure γ-H2AX foci induction in marine and freshwater bivalves (González-Romero et al., 2012). γ-H2AX response was confirmed in multiple tissue cell types (in both MG and DP) using standardized techniques in our laboratory on malignant human cells (Oommen et al., 2016a, 2016b), before the ^{32}P exposure studies. γ-H2AX optimisation in gill and digestive gland cells was performed using hydrogen peroxide (H_2O_2, 0, 5, or 500 µM

in PBS) as a reference agent (Dallas et al., 2013; Sarkar et al., 2015; Vernon and Jha, 2019). Briefly, tissues were digested as in section 2.2.1 and pooled to reduce inter-individual variability. Cell aliquots (150 µL) were transferred to tubes and spun (775 g, 2 min, 4 ^{o}C), once supernatant was discarded (leaving approx. 10 µL), H_2O_2 was added to the cellular pellet. Samples were then incubated (1 h, 4 ^{o}C, dark), spun (as before), supernatant removed, and cellular pellet was processed as detailed below.

Cells (100 µl, section 2.2.1) were secured onto coverslips using a slide centrifuge (Cytospin 4, Thermo Fisher Scientific Inc., Waltham, MA, USA, 140 g, 5 min), coverslips were then placed in individual wells of a multiwell plate (6 well plate, sterile, Greiner Bio-One, UK). Slides were chilled (20 min, 4 ºC) to allow adhering of cells and fixed with ice-cold Carnoys solution (20 min, 4 ºC, 75% methanol, 25% glacial acetic acid, 1 mL per well). Subsequent to fixation, coverslips were rinsed with PBS (Dulbecco, Fisher), in triplicate.

Cells were permeabilised (10 min, 0.5% Triton X-100 in PBS, room temp), blocked (1.5 h, normal goat serum, 60 µl per coverslip, G9023, SIGMA) and rinsed in triplicate with 0.1% Triton X-100/PBS. Following incubation (overnight, 4 ºC) with the primary antibody (60 µL per slide, 1:10000 in 0.1% Triton X-100/PBS, anti-GamaH2H [γ-H2AX]), cells were rinsed (in triplicate, 0.1% Triton X-100/PBS) and incubated in the dark with the secondary antibody (1 h, 60 µL per slides, 1:1000 in 0.1% Triton X-100/PBS, Anti-IgG secondary antibody, room temp). The slides were then rinsed as before. Procedural blanks were run alongside samples, with no primary antibody. Cells were counterstained with DAPI (1 µg 10 mL^{-1} PBS, 10 min, dark) and rinsed (in duplicate, DI water). Coverslips were gently removed from well plates, tilted to remove excess liquid and mounted onto labelled slides. Slides were scored using a fluorescence microscope (NIKON Epifluorescence 80i, 60x magnification), by

counting the number of foci in each of 50 cells per individual. As described by (Festarini et al., 2015), cell nuclei were located with an appropriate DAPI filter, and a FITC filter set for the FITC signal of the γ-H2AX primary antibody. All coded slides, including procedural blanks were scored blind.

2.2.5 Determination of transcriptional expression of key genes

2.2.5.1 RNA extraction and cDNA synthesis

Total RNA was extracted from gill and digestive gland tissues using the GenElute™ Mammalian Total RNA Miniprep Kit (RTN350, Sigma-Aldrich Company Ltd., UK), as described in details from previous studies published from our laboratory (Dallas et al., 2013, 2016, 2018). Briefly, tissue, lysis buffer (guanidine thiocyanate and 2-mercaptoethanol) and glass beads (2 mm, Merck, UK) were transferred into a microcentrifuge tube, and homogenised (FastPrep®, 30 s, 5 m/s) to form a smooth lysate, subsequent steps were in accordance to manufacturer's instructions. RNA concentration and purity of the samples were determined by UV spectroscopy (Nanodrop 3300, Thermo-Fisher, UK), total RNA was stored at −80 °C. 1 µg of total RNA from each tissue was used for cDNA synthesis with the Applied Biosystems High-Capacity cDNA reverse transcription kit (Fisher Scientific, UK) including RNase inhibitor.

2.2.5.2 Real-time Polymerase chain reaction (PCR)

Real-time polymerase chain reaction, or Quantitative PCR (qPCR) was performed to determine transcriptional expression of selected genes involved in stress responses in selected tissues of both the species (Table 2). Applied Biosystems StepOne Plus PCR System (Life Technologies, Carlsbad, CA, USA) with StepOneTM Software

(v2.2.2; Applied BioSystems), as described in details from earlier publications from our laboratory were used to perform these studies (Dallas et al., 2013, 2016, 2018) . Briefly, cDNA (1.9 µL), PowerUp™ SYBR™ Green Master Mix (7.5 µL), forward/reverse primers (0.03 µL/primer) and molecular grade water (5 µL) were added to a 96 well plate (MicroAmp™ Fast Optical 96-Well Reaction Plate, 0.1 mL) to make a total volume of 15 µL per well. Thermocycling conditions were as follows: 2 min, 95 °C; 40 cycles of 95 °C for 15 sec and 1 min, 60 °C. A dissociation curve (melt curve) was run to verify consistency of the PCR products.

Table 2. Gene and primers used for *M. galloprovincialis* and *D. polymorpha* in RT-PCR.

Gene	Short name	Forward primer	Reverse primer	GenBank Accession No.
		Mytilus galloprovincialis		
Actin	*act*	5' -GGGAGTCATGGTTGGTATGG- 3'	5' -TCAGAAGGACTGGGTGCTCT- 3'	AF157491
Elongation factor 1	*ef1*	5' -CACCACGAGTCTCTCCCAGA- 3'	5' -GCTGTCACCACAGACCATTCC- 3'	AF063420
Glutathione S-transferase	*GST*	5' -ATGGCTCTTTTCCTGCTTCA- 3'	5' -TTTGGCCAGTGTCCATGTTA- 3'	AF527010
Superoxide dismutase	*CuZn-sod*	5′ -TGCAGGATCACATTTCAACCCA-3′	5′ -TGTCTTGCTTAGCTCATGGCCA-3′	AJ581746
Catalase	*CAT*	5' -CACCAGGTGTCCTTCCTGTT- 3'	5' -CTTCCGAGATGGCGTTGTAT- 3'	AY743716
Heat-shock Protein 70	*HSP70*	5' -GGGTGGTGGAACTTTTGATG- 3'	5' -GCCGTTGAAAAAGTCCTGAA- 3'	AF172607
Heat-shock Protein 90	*HSP90*	5' -TCAGTGATGATCCTAGATTAGGCA- 3'	5' -CGTTCCTCTCTTTCCATCTGTAAC- 3'	AJ625655
		Dreissena polymorpha		
Actin	*act*	5' -CCTCACCCTCAAGTACCCCAT- 3'	5' -TTGGCCTTTGGGTTGAGTG- 3'	AF082863
Elongation factor 1	*ef1*	5' -CCACCAAAGGCAGCCAAGAG- 3'	5' -TGGGACGAGGTCAGCCATAC- 3'	AJ250733
Glutathione S-transferase	*GST*	5' -TCCGCTATATCTGCCTGGAC- 3'	5' -GCTCCTTCAGACCTGCTTTC- 3'	EF194203
Superoxide dismutase	*SOD*	5' -GACAGCATGGCTTCCATGTG- 3'	5' -AGATTCTGGGCCAGTCAGAG- 3'	AY377970
Catalase	*CAT*	5' -ACGGCTATGGAAGCCACACG- 3'	5' -AGGTCGCGCATCGCATAGTC- 3'	EF681763
Heat-shock Protein 70	*HSP70*	5' -TGTCCTGCTTGTGGATGTAG- 3'	5' -CGTGGTGAATGTCTGTGTAG- 3'	EF526096
Heat-shock Protein 90	*HSP90*	5' -TTGATCATCAATACTTTCTATTC- 3'	5' -ACACCAAACTGTCCAATCAT- 3'	GU433881a

2.3 Determination of ^{32}P and Cu concentration in water samples

2.3.1 Determination of ^{32}P in water samples using liquid scintillation counting

Water samples (including non-spiked salt/freshwater blank) were mixed with 4 mL scintillant (ScintLogic U, LabLogic Systems Ltd., UK) in vials (20 mL, Fisherbrand™ Borosilicate Glass) and left in dark for ~ 2 h prior to counting (Hidex 300SL). Samples were read for 10 sec, in triplicate. All samples were background corrected by blank subtracting, along with necessary decay adjustments. In accordance with (Jaeschke and Bradshaw, 2013), CPM values below the blanks were assigned an activity of 0.000.

2.3.2 Determination of Cu concentration in water samples using Inductively Coupled Plasma Mass Spectrometry (ICP-MS)

Water samples (1 mL) were spiked with 50 µL HCl immediately after extraction, and stored at room temperature until analysis, as described in detail in Dallas et al. (2013). Indium (115-In) and iridium (193-Ir) were added to samples as internal standards. Seawater samples were diluted 1:5 with DI water. Appropriate Cu standards were made to calibrate the instrument before and during analysis of samples, in accordance to Al-Subiai et al. (2011) and D'Agata et al. (2014). Using appropriate parameters (^{63}Cu and ^{65}Cu), standards and samples were run using X Series II ICP-MS (Plasma Quad PQ2 Turbo, Thermo Elemental, Winsford, UK) with PQ Vision 4.1.2 software. Procedural blanks were run every 10 samples.

2.4 Dosimetry and the ERICA tool

The Tier 2 assessment module of the ERICA tool was used for dose estimation, with ^{32}P chosen as one of the ERICA tool's default isotopes (Brown et al., 2008; Vernon et

al., 2018). Custom MG geometry parameters (i.e. mass, height, width, length) were adopted from Dallas et al. (2016), for DP, custom parameters (mean measurements from experimental mussels) were used for accurate dosimetry (Vernon et al., 2018). A radiation-weighting factor of 1 (ERICA tool's default for high energy beta emitters) was used. Concentration ratio was set to 0 as tissue activity concentrations (data from previous experiments, see below) were used (Vernon et al., 2018). Variable inputs required to calculate total dose rate per organism (μGy h^{-1}) were water activity concentration (Bq L^{-1}), the sediment-water distribution co-efficient (Kd, 0 L kg^{-1}, as no sediment was present in the experimental design), and the organism activity concentration, calculated as Bq kg^{-1}. The calculation and methodologies adopted for organism activity concentration has been described in more detail in our earlier studies (Vernon et al., 2018). From a previous experiment, the % of ^{32}P being accumulated into mussel tissues (whole-body and individual tissue) was calculated (e.g. 44% of ^{32}P in water is accumulated into 35 g of MG at 10 mGy d^{-1}). Using water activity concentrations (Bq L^{-1}) from the current exposure, ^{32}P activity concentration was determined in whole-body, gill and digestive gland (Bq in 35 g^{-1}, whole-body). This value was divided by total mussel wet weight (35 g, including shell) per beaker, and then multiplied by 1000 to acquire Bq kg^{-1}.

2.5 Statistical analysis

In accordance with Dallas et al. (2013, 2016), relative mRNA expression ratio (RER) of key genes (*sod, cat, gst, hsp70 and hsp90*) was quantified using REST (v 2009), from PCR efficiencies calculated using LinReg PCR software (version 11, Ramakers et al., 2003; Ruijter et al., 2009) and threshold cycle (Cq). Values were normalised to the geometric mean of Cq determined for reference genes actin (*act*) and elongation factor 1 (*ef1*), using control samples to calibrate.

All statistical analyses were carried out using the statistical software R (RStudio, R 3.4.3 GUI 1.70 El Capitan build (7463), https://www.r-project.org/). Data were checked for normality distribution (Shapiro-Wilk test) and homogeneity of variances (Levene's test), with visual examination of QQ-plots. The non-parametric Kruskal-Wallis test was used if assumptions were not met; comparison between treatment groups was determined using a Dunn's pairwise comparison with Bonferroni correction. Where assumptions were met, a one-way ANOVA was run with Tukey's post hoc tests. To compare between treatment groups, a Wilcoxon rank sum test with Holm-Bonferroni correction was used. Any correlation between variables was determined using a Pearson's correlation coefficient. Level of significance for all tests was set at $p < 0.05$ (*) and data presented as mean ± standard deviation, unless otherwise stated.

3 Results

During the exposure periods, no spawning or mortality of mussels occurred for either of the species. Metal (Cu) and ^{32}P concentrations, along with water quality measurements are presented in Table 1. Results of the ICP-MS and LSC analysis confirmed that achieved values were in line with expected concentrations across all treatments.

3.1 Whole-body and tissue specific dose rates

Dose rates for whole body and specific tissues (i.e. gill and digestive gland) are illustrated in Table 3. Whole body dose rates were 0.10, 0.97, 10.66 for MG and 0.08, 0.93, 10.32 mGy d^{-1} for DP, in line with predicted values. The highest dose rates were evident in digestive gland tissue, with rates around 39 (MG) and 31-fold (DP) higher than whole body dose in the 10 mGy d^{-1} treatment. In MG, whole body and gill tissue

dose rates were comparable. Whole-body and tissue activity concentrations (Bq g^{-1}) are detailed in our earlier study (Vernon et al., 2018).

Table 3. Table to show (a) the expected dose rates in mGy d^{-1} and (b) the average dose rate achieved in *M. galloprovincialis* and *D. polymorpha* whole-body, digestive gland and gill tissue (mGy d^{-1}). Values in bold are those above the ERICA tool screening value of 0.24 mGy d^{-1}.

		Av. Dose rate (mGy d^{-1})		
	Expected dose rate	Whole body	Digestive gland	Gill
M. galloprovincialis	0.1	0.10	**4.32**	0.06
	1	**0.97**	**39.12**	**0.78**
	10	**10.66**	**420**	**10.13**
D. polymorpha	0.1	0.08	**1.52**	**0.8**
	1	**0.93**	**3.84**	**1.74**
	10	**10.32**	**319.2**	**6.07**

3.2 Genotoxic response following *in vivo* exposures to ^{32}P

Fig. 2 shows the mean (+ S.D) % tail DNA damage, MN per 1000 cells and γ-H2AX induction in MG and DP gill cells, following exposure to varying ^{32}P concentrations for 10 days. All control treatments showed a low degree of damage across all biomarkers, indicative of good health in study species.

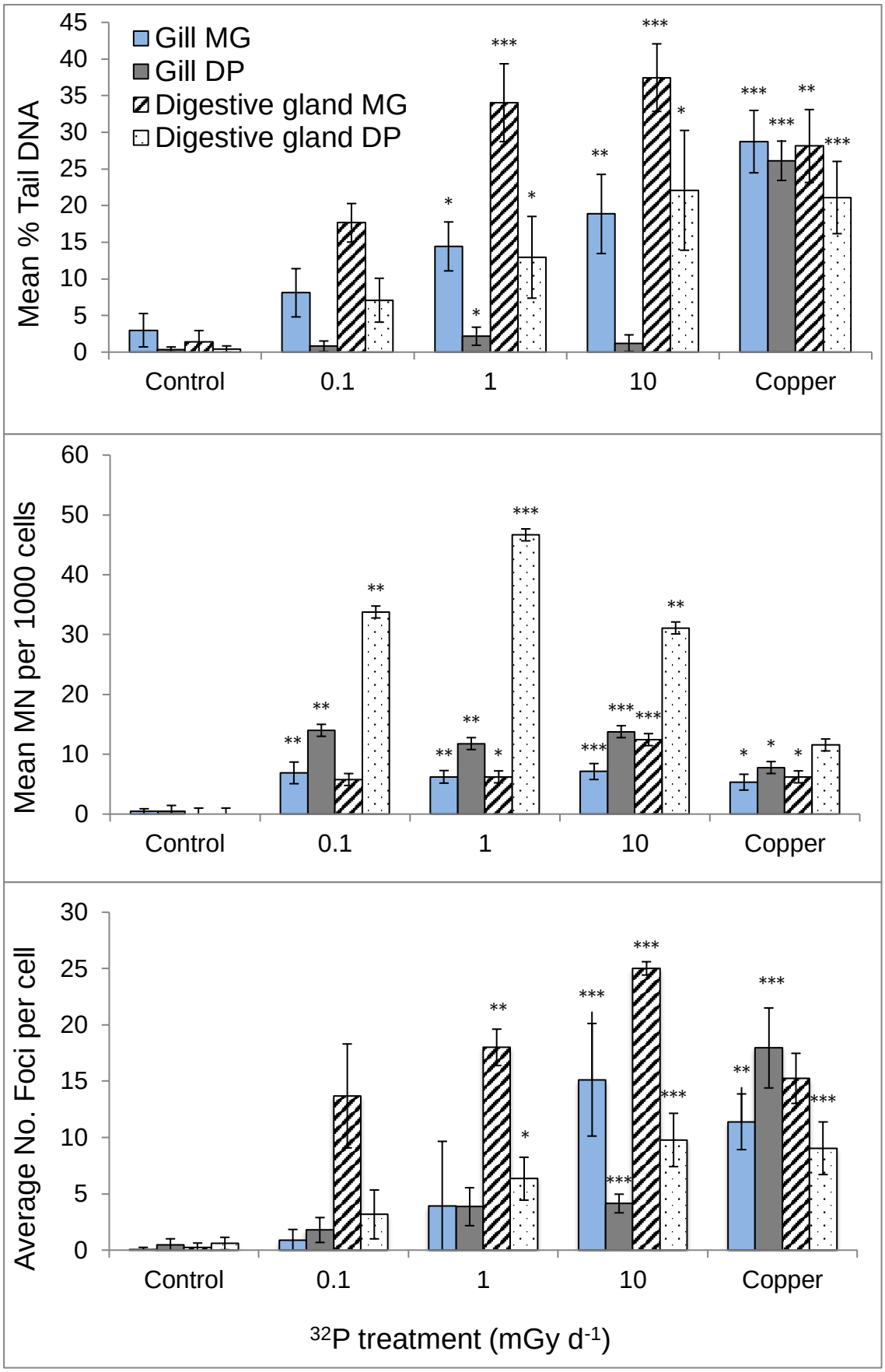

Figure 2. Genotoxic effects in *M. galloprovincialis* and *D. polymorpha* gill cells following a 10-day exposure to ^{32}P. Asterisks (*, ** or ***) are indicative of significant differences (p < 0.05, 0.01, 0.001) from the corresponding control. SD is standard deviation of mean data. n=9.

3.2.1 Comet assay to determine DNA strand breaks

The results indicate that in terms of DNA damage (% Tail DNA, Fig. 2), excluding DG gill, all tissues showed a significant dose dependant increase in response to ^{32}P ($p < 0.01$), particularly in MG tissue and DP digestive gland. Control samples showed low levels of damage, with tail DNA of around 1-2%. The highest level of damage was evident in MG digestive gland cells for both 1 and 10 mGy d^{-1} doses, with around 34-37% tail. MG tissue (gill and DG) showed greater DNA damage across all ^{32}P treatments when compared to the equivalent DP tissues ($p < 0.01$). There was no statistical difference between DNA damage for the 1 and 10 mGy d^{-1} doses, a trend also observed for MN and γ-H2AX formation across all tissues (apart from MG gill cells, γ-H2AX, $p < 0.05$).

3.2.2 Analysis of micronuclei (MN) induction

MN formation (Fig. 2) did not follow the dose-dependent response pattern that was evident for DNA damage (comet response) and γ-H2AX induction, while ^{32}P had a significant effect ($p < 0.001$) there was little difference between treatment groups. DP digestive gland showed significantly greater MN formation compared to MG digestive gland, gill and DP gill, especially for 1 mGy d^{-1} dose at 47 MN per 1000 cells. Similarly, MN induction in DP gill cells was higher than that in MG gill, across all treatments, however it was not significant ($p = 0.92$).

3.2.3 Induction of γ-H2AX foci

The 10 mGy d^{-1} dose produced the highest degree of damage across all species and tissues, in comparison to controls ($p < 0.001$). In keeping with DNA damage, the greatest number of γ-H2AX foci was in MG digestive gland cells, across all ^{32}P

treatments with around 13-25 foci per cell. On average, the number of foci in MG digestive gland was 3-4 fold greater than in DP digestive gland cells ($p < 0.01$). Following exposure to a dose of 0.10 mGy d^{-1}, there was no significant increase in γ-H2AX or DNA damage, in any of the tissues of either species.

3.3. Transcriptional expression of key genes

PCR efficiencies for studied genes were: *actin* (*act*): 1.79, *elongation factor 1* (*ef1*): 1.79, *catalase* (*cat*): 1.81, *glutathione-s-transferase* (*gst*): 1.81, *superoxide dismutase* (*sod*): 1.80, *heat shock protein 70* (*hsp70*): 1.75 and *heat shock protein 90* (*hsp90*): 1.83 for MG, and *act:* 1.80, *ef1:* 1.79, *cat:* 1.82, *gst:* 1.79, *sod:* 1.78 and *hsp70:* 1.81 for DP. *hsp90* data is not included for DP as the assay failed to amplify. Relative gene expression of the selected genes are presented in figure 5, there was limited variation across all biological tissue and species. Gene *hsp70* was significantly upregulated in DP gill following ^{32}P exposure ($p < 0.05$), along with *gst* in the 1 mGy d^{-1} treatment, however to a limited degree.

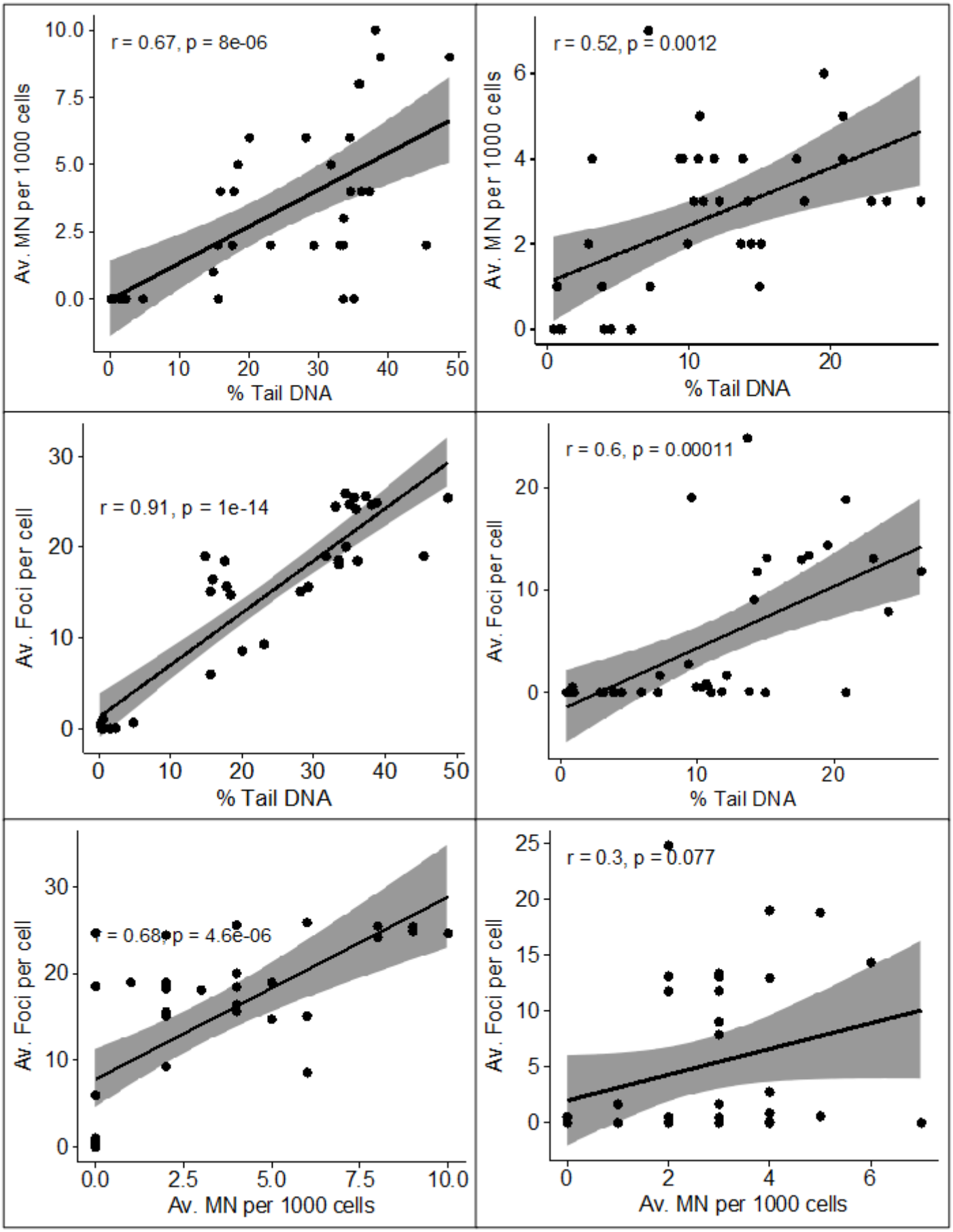

Figure 3. Pearson's correlation analyses of: (top to bottom) % tail DNA and induction of MN, % tail DNA and γ-H2AX foci, and induction of MN and γ-H2AX foci. *M. galloprovincialis* digestive gland (left) and *M. galloprovincialis* gill (right). *n*=9.

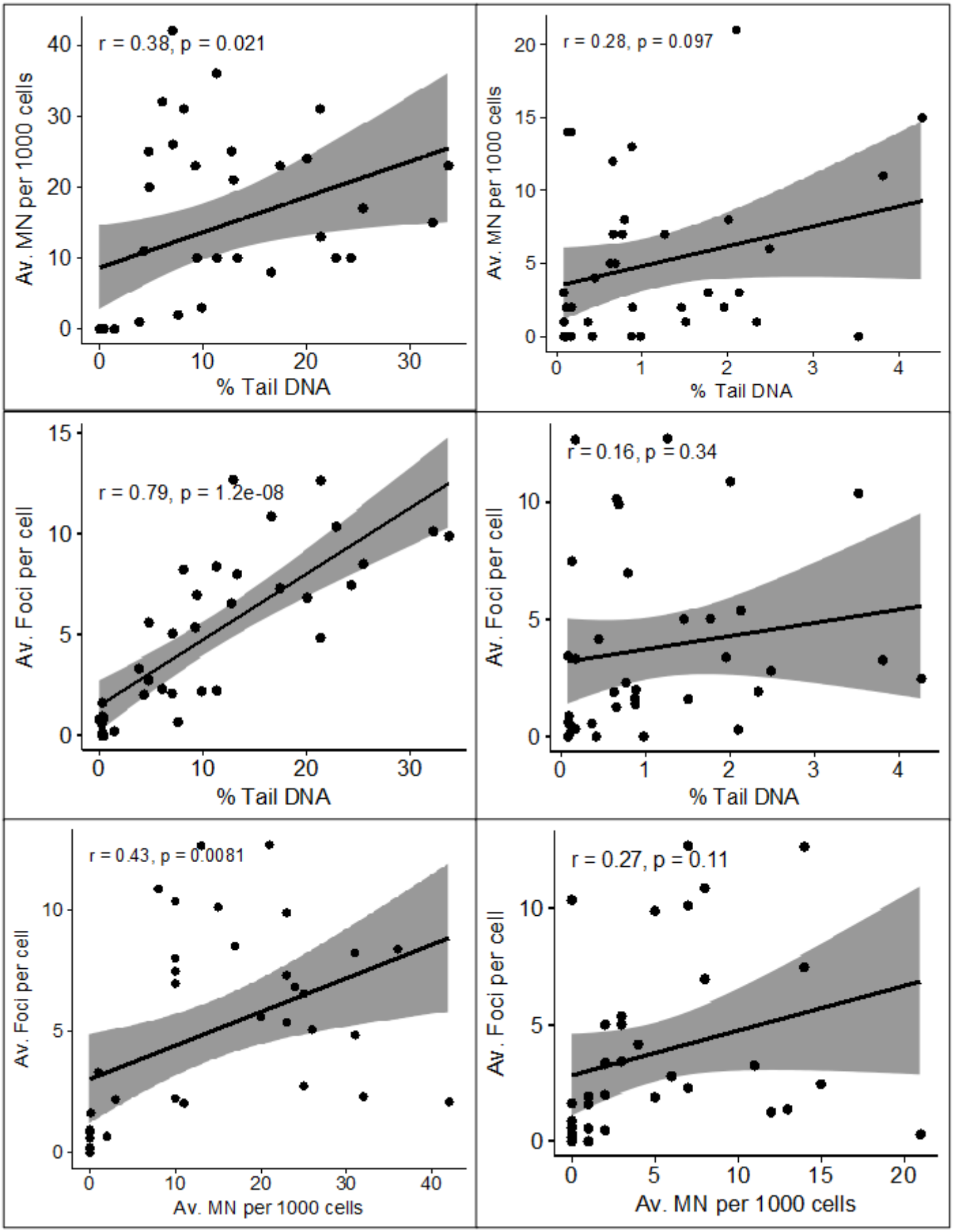

Figure 4. Pearson's correlation analyses of: (top to bottom) % tail DNA and induction of MN, % tail DNA and γ-H2AX foci, and induction of MN and γ-H2AX foci. *D. polymorpha* digestive gland (left) and *D. polymorpha* gill (right). *n*=9.

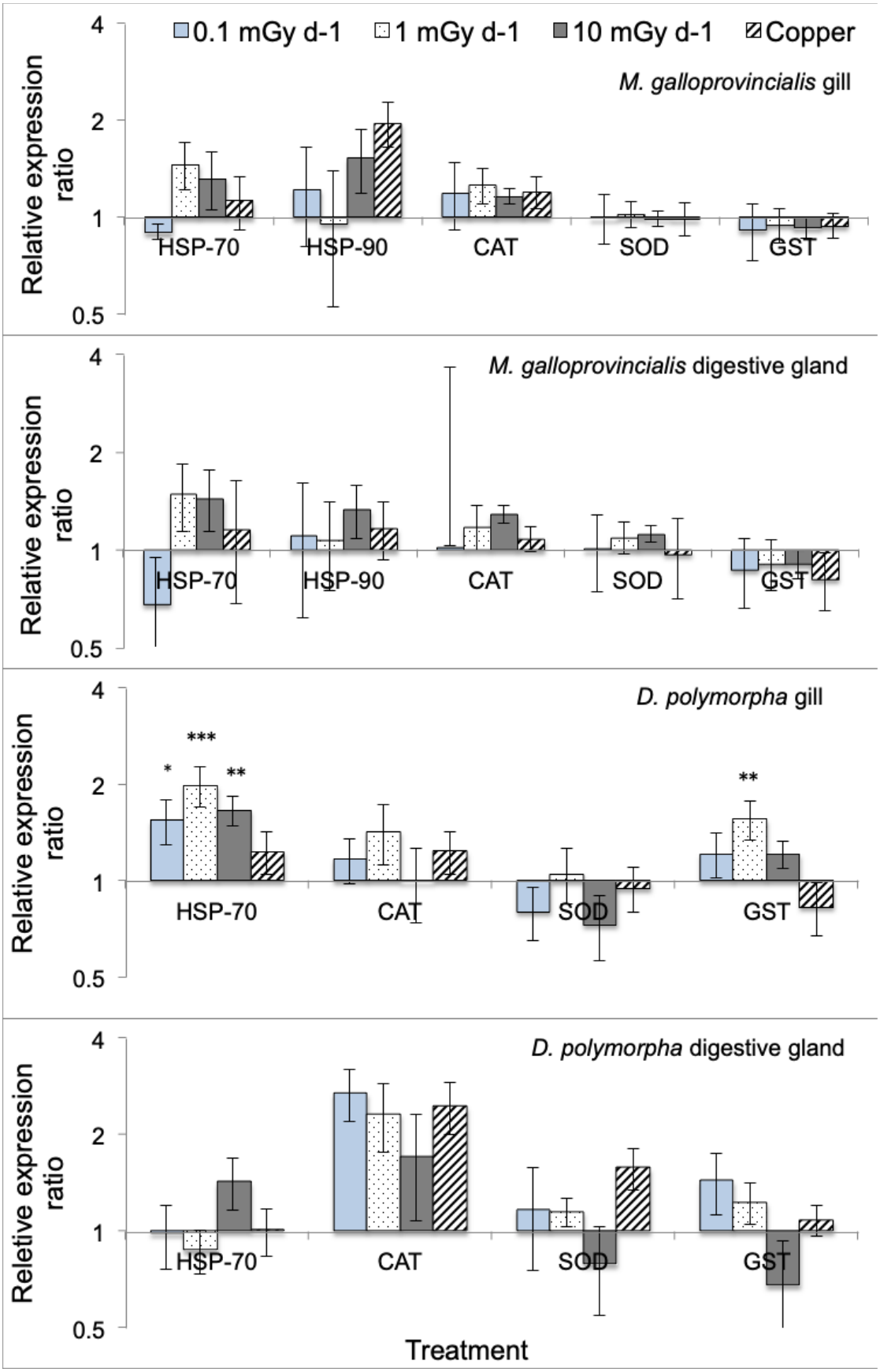

Figure 5. Relative expression ratios (RER) of key genes in *M. galloprovincialis* and *D. polymorpha* gill and digestive gland cells following a 10-day exposure to ^{32}P. Data are normalised for reference genes (*ef1, actin*) and controls. Error bars indicate the 95% confidence intervals. Asterisks (*, ** or ***) are indicative of significant differences ($p <$ 0.05, 0.01, 0.001) from the corresponding control. n=9.

4 Discussions

4.1 Dosimetry and dose-response relationship

Our study investigated the tissue specific effects of IR following exposure to ^{32}P on marine and freshwater bivalves, using a multi-biomarker approach. It is important to note that in the current study, ^{32}P was introduced in a highly bioavailable form (i.e. radiolabelled ATP). The observed biological responses may be reflective of this form of radioactive phosphorus (Vernon et al., 2018). Our study firstly suggests that gill and digestive gland tissues are sensitive and reliable cell types for assessing IR-induced damage, alongside haemocytes which are predominantly chosen as target cell types to study biological responses (Jha et al., 2005, 2006; Jaeschke et al., 2015; Dallas et al., 2016; Pearson et al., 2018). Secondly, our study has highlighted the necessity to evaluate response in several organs, as greater ^{32}P activity levels within digestive gland tissue in particular has induced a greater genotoxic response (Fig 2). Whole body dose rates (Table 3) in this instance are likely to mask the potential biological effect of ^{32}P. At dose rates below the screening value of 10 μGy h^{-1} (0.24 mGy d^{-1}) (Andersson et al., 2008, 2009), whole body dose estimations (MG 0.10; DP 0.08 mGy d^{-1}) would suggest a minimal risk to individual or population. However, MG digestive gland dose as an example (4.32 mGy d^{-1}), is 43-fold greater than whole body. As suggested by Jaeschke et al. (2011) and Jha (2008), it is important to determine tissue specific effects in response to a wide range of contaminants. Successful environmental protection is dependent on the preservation of natural populations (e.g. population size and growth rate, structure). Whilst not within the scope of this study, there is a need to understand whether IR-induced effects at subcellular levels, focussing on particular tissues can impact higher levels of biological organisation (i.e. community, population, and ecosystem). Establishing a link between sub-lethal

molecular or biomarker responses to higher levels of biological organisations have however been a challenging task (Jha, 2008). In recent years, adoption of 'Adverse Outcome Pathway (AOP)' has been suggested to address this issue where results obtained from different organisms and at different levels of biological organisations can be synthesized to extrapolate the information to assess the risk at population or community levels (Ankley et al., 2010). This would aid the implementation of adequate protection policies and suitable radiation benchmarks, or could indicate where assumptions made when making such policies are insufficient.

4.2 ^{32}P induced genotoxic response in gill and digestive gland cells

4.2.1 Comet assay to determine DNA strand breaks

The present study revealed significant DNA damage (as % Tail DNA) in MG gill tissue and the digestive glands of both species, suggesting strong correlations between dose rate and the response. Our results are in line with previous studies where exposure to doses between 12-485 µGy h^{-1} (tritiated water, HTO) induced significant damage in haemocytes of *Mytilus* sp. (Jha et al., 2005, 2006; Dallas et al., 2016; Pearson et al., 2018). In both species the highest DNA damage was evident in digestive gland cells, most likely due to high ^{32}P accumulation, and therefore dose rate. To our knowledge, only a few radiobiological studies have investigated IR-induced response in digestive organs. This is despite the key role of these organs in metabolism, immune defence, and as a primary sink for many aquatic contaminants (McDonald et al., 1993; Cartier et al., 2004; Dimitriadis et al., 2004; Banni et al., 2017; Faggio et al., 2018; Sforzini et al., 2018). No significant level of DNA damage is evident at dose rates of 0.10 mGy d^{-1} in either tissue or species. This is in contrast to Jha et al. (2006), where low doses of tritium (0.30 mGy d^{-1}, 96 h) induced a 2.8-fold increase in damage compared to control cells in haemocytes of mussels. This trend was also observed in Zebrafish (*Danio rerio*,

96 hpf larvae), where exposure to low dose-rates (^{137}Cs, 0.80 mGy d^{-1}) caused significantly increased damage (Gagnaire et al., 2015). The relatively low dose rate to DP gill cells (Table 3) resulted in minimal damage to DNA across all treatments, with a slight increase for 1 mGy d^{-1} dose ($p < 0.05$). Despite the lower dose rate to MG gill compared to DP gill cells (0.1 and 1 mGy d^{-1}), DNA damage was noted (~7-15 % tail DNA). Disparity may be down to numerous factors, including differential sensitivity between cell types or species, radionuclide properties (e.g. linear energy transfer: LET values), absorbed dose, exposure length and physiological factors (i.e. reproductive stage, metabolism, health status) (Nalepa et al., 1991; Jha, 2008; Pearson et al., 2018). As previously noted, ^{32}P incorporates directly onto the ribose-phosphate backbone of replicating DNA and isotopic decay (^{32}P to ^{32}S) breaks the initial strand (SSB), and by close proximity emitted elections can cause DSBs. This will result in a higher proportion of strand breaks compared to other beta emitters (i.e. ^{90}Y, ^{131}I) (Cheng et al., 2015). The comet assay in this instance is useful in showing current, non-specific (i.e. single or DSBs) DNA damage, often regarded as more sensitive when combined with other biomarkers (Frenzilli et al., 2009). Future studies would benefit from measuring DNA damage post exposure at multiple time points, as to monitor possible DNA repair in different cell types. This would be particularly relevant for MG digestive gland cells, where a high degree of DNA damage is paralleled ($r = 0.91$, $p < 0.001$) by increased γ-H2AX foci, suggesting the recruitment of DNA repair proteins (Kuo and Yang, 2008).

4.2.2 Induction of γ-H2AX foci

IR has the potential to damage cellular DNA and, to maintain genomic integrity and function, repair enzymes/mechanisms are required (Hoeijmakers, 2001; Sancar, 2004). The long-term biological impact of ^{32}P is dependent on the efficiency of such

DNA repair mechanisms, as unrepaired DNA lesions may result in genetic mutation, leading to cancer formation or cell death. Immunostaining techniques such as the H2AX assay can be utilised as sensitive markers to compare DNA DSBs in cells, and therefore DNA damage response (DDR). Gamma-H2AX (γ-H2AX) is a histone alteration, which appears rapidly and forms foci at sites of DNA DSBs, evolutionary this biological response is highly conserved (Foster and Downs, 2005; Pereira et al., 2011; González-Romero et al., 2012). The phosphorylated H2AX protein, γ-H2AX plays an important role in DNA damage signalling and repair, along with activation of checkpoint proteins and apoptosis (Fragkos et al., 2009; Podhorecka et al., 2010). Foci are utilised as a direct measure of repair as DSBs are represented in a 1:1 manner (Kuo and Yang, 2008). γ-H2AX foci induction following ^{32}P exposure (111 kBq, 24 h) has been displayed in HeLa S3 cells, mouse BALB/c CRL2836 cells and other malignant cell lines, along with other biological responses (Cheng et al., 2015; Oommen et al. 2016a, 2016b).

In terms of aquatic biota, γ-H2AX induction has been noted at dose rates of 70-550 mGy d^{-1} in Zebrafish ZF4 cells and embryos, in response to ^{137}Cs exposure (Pereira et al., 2011, 2014). In Medaka (*Oryzias latipes*) fish erythrocytes, a high frequency of γ-H2AX foci (2 h, 39.9 ± 45.05) were noted following an acute exposure (15 Gy) to ^{137}Cs, and in line with our study, were well correlated with DNA damage (as measured by the comet assay) (Sayed et al., 2017). The present study suggests that mussels are able to employ repair mechanisms following ^{32}P induced DNA damage, while no significant increase in γ-H2AX formation was evident at 0.10 mGy d^{-1}, a dose dependant response was demonstrated overall. If we compare data obtained from comet and γ-H2AX assays, several similarities are apparent, and a good correlation is evident between all end-points (all but DP gill cells). γ-H2AX foci represent DSBs in

a 1:1 manner (Kuo and Yang, 2008), the strong correlation between comet and γ-H2AX assays in our study suggests that the majority of DNA damage evident is in the form of DSBs, as opposed to SSBs, alkali-labile sites or DNA cross-links.

γ-H2AX is dephosphorylated rapidly after DNA repair and is therefore time-dependant. Foci peak in size at around 30 min, and decrease in number over time (Sedelnikova et al., 2003; Ivashkevich et al., 2011, 2012). As noted by Sayed et al. (2017), γ-H2AX foci per cell (Medaka erythrocytes) peaked 2 h after exposure, and declined steadily over time (24 h). As suggested, a minimum of 50-100 cells should be counted per sample for γ-H2AX foci per cell (Redon et al., 2009; Oommen et al., 2016b). This study is therefore limited by inconsistent *n* numbers analysed per sample. Whilst care was taken to process the tissues for analysis immediately after exposure, in our study it is possible that all end-points would vary over time. Monitoring during, immediately after, and h/days post exposure would allow for a more clear indication of persistence or repairable effects.

Differing repair capacities are evident between the digestive glands of MG and DP. In terms of MG digestive gland, a high degree of DNA damage and γ-H2AX foci induction (~ 25 foci/cell, 10 mGy d^{-1}), combined with relatively low MN induction suggests efficient DNA repair mechanisms. In comparison, in DP digestive gland γ-H2AX foci induction is 2.5-4.3 fold lower than MG, but MN formation is significantly greater. This could indicate a less efficient DNA repair mechanism, or that the system was overwhelmed. It is important to note that γ-H2AX foci form at both unprogrammed and programmed DSBs. Due to low foci number in control samples (~0.3 foci/cell), we are confident in attributing foci formation to ^{32}P exposure in our study (Sedelnikova et al., 2003; Revet et al., 2011). To avoid misinterpretation of results, it is important that

baseline levels of cellular DSBs are optimised and determined prior to exposures to contaminants and by using appropriate controls.

4.2.3 Analysis of micronuclei (MN) induction

MN represent fragments of chromosomes or whole chromosome formed either via misrepair of DNA DSBs or due to malfunctioning of microtubules (Fenech et al., 2011; Bolognesi and Fenech, 2012). The capacity of IR to induce MN has previously been reported in bivalves (*M. edulis*) and fish (*Catla catla, Cyprinus carpio, Oryzias latipes*) (Jha et al., 2005, 2006; Anbumani and Mohankumar, 2012; Jaeschke et al., 2015; Kumar et al., 2015; Sayed et al., 2017; Hurem et al., 2018). Our results suggest that MN formation is the most sensitive endpoint to ^{32}P, as significant MN formation was present even at the lowest dose (0.10 mGy d^{-1}, all but MG digestive gland). DP digestive gland cells had a vast number of MN in comparison to all other ^{32}P treatments at around 31-47 MN/1000 cells. This suggests that DNA damage overwhelmed the repair capacity of the cells, resulting in less reversible, more permanent effects.

A slight correlation is evident between DNA damage and increased MN frequency in all but DP gill (MG digestive gland: $r = 0.67$, $p < 0.001$, MG gill: $r = 0.52$, $p < 0.01$, DP digestive gland: $r = 0.38$, $p < 0.021$, Fig 3 and 4). This is in contrast to previous studies where strong positive correlations are noted (Bolognesi et al., 2004; Hagger et al., 2005; Jha et al., 2005; Canty et al., 2009; Kumar et al., 2015). While DNA damage was relatively low in DP gill, there was significant MN induction (at around 13 MN per 1000 cells) across all ^{32}P treatments. The lack of correlation between end points measured in DP gill may be a result of DNA-DNA or DNA protein crosslinks that inhibit tail migration during the comet assay (Hartmann et al., 2001; Klobučar et al., 2003). No significant variation was evident between ^{32}P treatments, and there is little distinction between species, cell type, or treatment, with MN frequency ranging

between 6-14 MN/1000 cells (excluding DP digestive gland). While the reason for this is unclear, differing results suggest varying MoA's between beta-emitting radionuclides (tritium, ^{32}P) on the DNA in mussels. Our study clearly shows the benefit of adopting a multi-biomarker approach in measuring IR-induced genetic damage. The combination of biomarkers aids the detection of differing aspects of genotoxicity (DNA repair and response) and clastogenicity (Jha et al., 2005; Araldi et al., 2015; Kumar et al., 2015).

4.3 Transcriptional expression of key genes

While genotoxic response to ^{32}P was evident in both species, there was little change in genes involved in cell stress defence mechanisms (protein folding or regulation of oxidative stress). Slight up-regulation of *hsp70* (all ^{32}P treatments, $p < 0.05$) and *gst* (1 mGy d^{-1}, $p < 0.001$) was noted in DP gill, albeit to a relatively limited degree.

IR generates reactive oxygen species (ROS) via the radiolysis of water (Barillet et al., 2011; Graupner et al., 2016). To minimise the detrimental effects of ROS, antioxidant enzymes such as *sod, cat* and *gst* are employed. It could be expected that genes involved with oxidative stress response, detoxification and/or cellular defence would be upregulated when exposed to IR. This was noted following acute exposure to ^{137}Cs in *Kryptolebias marmoratus* embryos, where antioxidant enzyme-coding genes (e.g. *gst, cat, mn-sod, cu/zn-sod*) were significantly upregulated at 5 Gy dose of ^{137}Cs gamma-rays (Rhee et al., 2012). However, our findings are in line with Devos et al. (2015) who reported significant genotoxic response (i.e. DNA damage, as measured by the comet assay) following exposure of *C. gigas* to tritium (0.07-1.1 mGy d^{-1}), but no change in gene expression levels (*hsp70, hsp90, hsc72, gst, mdr, cyp1a, sod, mt1&2 and p53*). This was also noted in MG gill cells following exposure to tritium (7 d, ~0.36 mGy d^{-1}), where DNA damage significantly increased ($p < 0.05$) in comparison

to control treatments, but gene expression levels remained unchanged (slight increase in *hsp70-1* and *rad51,* 72 h) (Dallas et al., 2016). However, after 3 days (72 h, ~0.36 mGy d^{-1}) significant upregulation was noted in all genes (*hsp70-1, hsp70-2, hsp90, mt20, p53, rad51*) (Dallas et al., 2016), suggesting time as an important factor in the transcriptional expression of genes. As suggested by Devos et al. (2015), the lack of change noted at a molecular level may suggest different sensitivities for end points, or disparity in the MoA of toxicity. It is possible that evident genomic damage resulted from direct interaction of ^{32}P with DNA, either through isotopic decay or the subsequent release of high-energy beta particles, and to a lesser degree via the generation of ROS.

Our gene expression analysis included a limited number of stress response genes, as the current study was limited to readily available gene sequences in both species. Future studies would benefit from studying a wider range of genes, particularly those involved in DNA damage and repair (i.e. *p53, ogg1*, *rad51*), or via a more open ended approach. This could include a high-throughput transcriptomic (e.g. microarrays, RNAseq) or proteomic approaches (Banni et al., 2017; Barranger et al., 2019), which allows the measurement of expression levels in thousands of genes/proteins. This would allow identification of early IR-induced responses, and would aid the identification of mechanisms involved in an organism's toxicity response to IR.

4.4 Environmental implications and future research

While ^{32}P occurs in small quantities in the environment, when accumulated into biological tissue, especially under chronic exposure scenarios, it is able to induce significant genomic damage. The marine and freshwater species chosen for this study represent suitable models to investigate ^{32}P induced toxicity. The multi-species approach adopted here could be regarded as more robust and realistic than single-

species experiments (Chapman, 2002; Solomon and Sibley, 2002; Canty et al., 2009; Schnug et al., 2014). Due to possible variations in ^{32}P speciation, and therefore bioavailability between salt and freshwater, we are unable to directly compare the study species. We are however able to establish a genotoxic response in both MG and DP, even at relatively low ^{32}P concentrations. Increased genomic instability may ultimately have a detrimental effect at higher levels of biological organization, from individual to long-term population level effects (Jha, 2008).

In the natural environment radionuclides are part of a complex mix of contaminants that can place combined pressure on the biota. Future study would benefit from: (a) combined field and laboratory studies, (b) laboratory experiments using a more realistic, flow-through exposure set-up (to note, due to health, safety, logistical and economic reasons a static exposure was utilised in this study), (c) multi-stressor and/or multi-species exposures, and (d) use of a wide range of radionuclides and exposure conditions. Knowledge of the behaviour, transfer and biological impact of radionuclides within aquatic systems allows for the development of adequate management and protective strategies.

5 Conclusions

Adopting the guidelines for recommended radiation screening dose likely to exist in natural environment, especially under chronic exposure scenarios, our study adds to very limited amount of available information on the effects of short-lived radionuclides on aquatic invertebrates. Our study also demonstrated that ^{32}P produces a measurable internal dose rate, which can be linked more accurately with novel biological responses. A greater tissue concentration for ^{32}P was paralleled by increased dose rates and consequent biological damage in two anatomically similar bivalve species. In terms of DNA damage and DDR, the marine species appeared to

be slightly more sensitive on an immediate, short-term level, possibly due to greater accumulation rates. As observed in this study, we do not always expect a typical or conventional dose–dependent response for all the endpoints determined. This low-dose, chronic study is the first to adopt a multi-species, multi-biomarker approach in investigating tissue specific ^{32}P induced biological response, along with dose-response relationships. This approach could be readily adopted to study impact of other radionuclides either alone or in combination with other environmental stressors for improved management of the environment.

Cells Acknowledgements

We thank Mr Nick Crocker, Dr Alex Taylor and Prof William Blake (University of Plymouth) for their technical assistance and advice during experimentation involving use of radionuclides. We also thank Prof Jim Smith (University of Portsmouth) for assistance with respect to application of the ERICA tool. Staff at the University of Exeter Medical School, Exeter are also thanked for use of their liquid scintillation counter. This work was jointly funded by the Natural Environment Research Council (NERC), the Environment Agency (EA) and Radioactive Waste Management Limited (RWM) under the Radioactivity and the Environment (RATE) programme (Grant no.: NE/L000393/1).

Author Contribution: ELV: Conceptualisation, Data curation, Formal analysis, Methodologies, Writing-Original Draft; TPB: Methodology, Writing- Review & editing;

ANJ: Conceptualisation, Formal analysis, Funding acquisition, Project administration, Resources, Supervision, Writing- Review and editing

Declarations of Interest: The authors declare no conflict of interest.

References

Al-Subiai, SN., Arlt, VM., Frickers, PE., Readman, JW., Stolpe, B., Lead, JR., Moody, AJ., Jha, AN., 2012. Merging nano-genotoxicology with eco-genotoxicology: An integrated approach to determine interactive genotoxic and sub-lethal toxic effects of C60 fullerenes and fluoranthene in marine mussels, *Mytilus* sp. Mutation Research/Genetic Toxicology and Environmental Mutagenesis 745: 92-103 doi https://doi.org/10.1016/j.mrgentox.2011.12.019

Al-Subiai, SN., Moody, AJ., Mustafa, SA., Jha, AN., 2011. A multiple biomarker approach to investigate the effects of copper on the marine bivalve mollusc, *Mytilus edulis*. Ecotoxicology and Environmental Safety 74: 1913-1920 doi http://dx.doi.org/10.1016/j.ecoenv.2011.07.012

AlAmri, OD., Cundy, AB., Di, Y., Jha, AN., Rotchell, JM., 2012. Ionizing radiation-induced DNA damage response identified in marine mussels, *Mytilus* sp. Environmental Pollution 168: 107-112 doi http://dx.doi.org/10.1016/j.envpol.2012.04.015

Anbumani, S., Mohankumar, MN., 2012. Gamma radiation induced micronuclei and erythrocyte cellular abnormalities in the fish *Catla catla*. Aquat Toxicol 122-123: 125-132 doi 10.1016/j.aquatox.2012.06.001

Andersson, P., Beaugelin-Seiller, K., Beresford, N., Copplestone, D., Della Vedova, C., Garnier-Laplace, J., Howard, B., Howe, P., Oughton, D., Wells Whitehouse, CP., 2008. Numerical benchmarks for protecting biota from radiation in the environment: Proposed levels, underlying reasoning and recommendation

Andersson, P., Garnier-Laplace, J., Beresford, NA., Copplestone, D., Howard, BJ., Howe, P., Oughton, D., Whitehouse, P., 2009. Protection of the environment from ionising radiation in a regulatory context (protect): proposed numerical benchmark values. J Environ Radioact 100: 1100-1108 doi 10.1016/j.jenvrad.2009.05.010

Ankley, G.T., Bennett, R.S., Erickson, R.J., Hoff, D.J., Hornung, M.W., Johnson, R.D., Mount, D.R., Nichols, J.W., Russom, C.L., Schmieder, P.K., Serrrano, J.A., Tietge, J.E.,Villeneuve, D.L., 2010. Adverse outcome pathways: a conceptual framework to support ecotoxicology research and risk assessment. Environ. Toxicol. Chem. 29, 730–741. doi.org/10.1002/etc.34.

Araldi, RP., de Melo, TC., Mendes, TB., de Sá Júnior, PL., Nozima, BHN., Ito, ET., de Carvalho, RF., de Souza, EB., de Cassia Stocco, R., 2015. Using the comet and micronucleus assays for genotoxicity studies: A review. Biomedicine & Pharmacotherapy 72: 74-82 doi https://doi.org/10.1016/j.biopha.2015.04.004

Bahrami, S., Drabløs, F., 2016. Gene regulation in the immediate-early response process. Advances in Biological Regulation 62: 37-49 doi https://doi.org/10.1016/j.jbior.2016.05.001

Banni, M., Sforzini, S., Arlt, VM., Barranger, A., Dallas, LJ., Oliveri, C., Aminot, Y., Pacchioni, B., Millino, C., Lanfranchi, G., Readman, JW., Moore, MN., Viarengo, A., Jha, AN., 2017. Assessing the impact of Benzo[a]pyrene on Marine Mussels: Application of a novel targeted low density microarray complementing classical biomarker responses. PLOS ONE 12: e0178460 doi 10.1371/journal.pone.0178460

Barranger, A., Rance, GA., Aminot, Y., Dallas, LJ., Sforzini, S., Weston, NJ., Lodge, RW., Banni, M., Arlt, VM., Moore, MN., Readman, JW., Viarengo, A., Khlobystov, AN., Jha, AN., 2019. An integrated approach to determine interactive genotoxic and global gene expression effects of multiwalled carbon nanotubes (MWCNTs) and benzo[a]pyrene (BaP) on marine mussels: evidence of reverse 'Trojan Horse' effects. Nanotoxicology: 1-20 doi 10.1080/17435390.2019.1654003

Barillet, S., Adam-Guillermin, C., Palluel, O., Porcher, JM., Devaux, A., 2011. Uranium bioaccumulation and biological disorders induced in zebrafish (*Danio rerio*) after a depleted uranium waterborne exposure. Environmental Pollution 159: 495-502 doi http://dx.doi.org/10.1016/j.envpol.2010.10.013

Bayliss, CR., Langley, KF., 2003. Chapter 2 - Ionising Radiation and its Control. In: Bayliss CR, Langley KF (eds) Nuclear Decommissioning, Waste Management, and Environmental Site Remediation. Butterworth-Heinemann, Burlington, pp 23-40
Bayne, BL., 1976. Marine mussels: their ecology and physiology. Cambridge University Press
Beyer, J., Green, NW., Brooks, S., Allan, IJ., Ruus, A., Gomes, T., Bråte, ILN., Schøyen, M., 2017. Blue mussels (*Mytilus edulis* spp.) as sentinel organisms in coastal pollution monitoring: A review. Marine Environmental Research 130: 338-365 doi https://doi.org/10.1016/j.marenvres.2017.07.024
Binelli, A., Della Torre, C., Magni, S., Parolini, M., 2015. Does zebra mussel (*Dreissena polymorpha*) represent the freshwater counterpart of Mytilus in ecotoxicological studies? A critical review. Environmental Pollution 196: 386-403 doi http://dx.doi.org/10.1016/j.envpol.2014.10.023
Bolognesi, C., Buschini, A., Branchi, E., Carboni, P., Furlini, M., Martino, A., Monteverde, M., Poli, P., Rossi, C., 2004. Comet and micronucleus assays in zebra mussel cells for genotoxicity assessment of surface drinking water treated with three different disinfectants. Science of The Total Environment 333: 127-136 doi https://doi.org/10.1016/j.scitotenv.2004.05.018
Bolognesi, C., Fenech, M,. 2012. Mussel micronucleus cytome assay. Nat Protocols 7: 1125-1137
Brown, JE., Alfonso, B., Avila, R., Beresford, NA., Copplestone, D., Pröhl, G., Ulanovsky, A., 2008. The ERICA Tool. Journal of Environmental Radioactivity 99: 1371-1383 doi http://dx.doi.org/10.1016/j.jenvrad.2008.01.008
Canesi, L., Frenzilli, G., Balbi, T., Bernardeschi, M., Ciacci, C., Corsolini, S., Della Torre, C., Fabbri, R., Faleri, C., Focardi, S., Guidi, P., Kočan, A., Marcomini, A., Mariottini, M., Nigro, M., Pozo-Gallardo, K., Rocco, L., Scarcelli, V., Smerilli, A., Corsi, I., 2014. Interactive effects of n-TiO2 and 2,3,7,8-TCDD on the marine bivalve *Mytilus galloprovincialis*. Aquatic Toxicology 153: 53-65 doi http://dx.doi.org/10.1016/j.aquatox.2013.11.002
Canty, MN., Hutchinson, TH., Brown, RJ., Jones, MB., Jha, AN., 2009. Linking genotoxic responses with cytotoxic and behavioural or physiological consequences: Differential sensitivity of echinoderms (*Asterias rubens*) and marine molluscs (*Mytilus edulis*). Aquatic Toxicology 94: 68-76 doi http://dx.doi.org/10.1016/j.aquatox.2009.06.001
Cartier, S., Pellerin, J., Fournier, M., Tamigneaux, E., Girault, L., Lemaire, N., 2004. Use of an index based on the blue mussel (*Mytilus edulis* and *Mytilus trossulus*) digestive gland weight to assess the nutritional quality of mussel farm sites. Aquaculture 241: 633-654 doi http://dx.doi.org/10.1016/j.aquaculture.2004.08.015
Carvalho, FP., 2018. Radionuclide concentration processes in marine organisms: A comprehensive review. Journal of Environmental Radioactivity 186: 124-130 doi https://doi.org/10.1016/j.jenvrad.2017.11.002
Chapman. PM., 2002. Integrating toxicology and ecology: putting the “eco” into ecotoxicology. Marine Pollution Bulletin 44: 7-15 doi https://doi.org/10.1016/S0025-326X(01)00253-3
Cheng, Y., Kiess, AP., Herman, JM., Pomper, MG., Meltzer, SJ., Abraham, JM., 2015. Phosphorus-32, a Clinically Available Drug, Inhibits Cancer Growth by Inducing DNA Double-Strand Breakage. PLOS ONE 10: e0128152 doi 10.1371/journal.pone.0128152
Cherry, SR., Sorenson, JA., Phelps, ME., 2012. chapter 3 - Modes of Radioactive Decay. In: Cherry SR, Sorenson JA, Phelps ME (eds) Physics in Nuclear Medicine (Fourth Edition). W.B. Saunders, Philadelphia, pp 19-30
Cheung, VV., Depledge, MH., Jha, AN., 2006. An evaluation of the relative sensitivity of two marine bivalve mollusc species using the Comet assay. Marine Environmental Research 62: S301-S305 doi https://doi.org/10.1016/j.marenvres.2006.04.053
Czapla-Masztafiak, J., Szlachetko, J., Milne Christopher, J., Lipiec, E., Sá, J., Penfold Thomas, J., Huthwelker, T., Borca, C., Abela, R., Kwiatek Wojciech, M., 2016.

Investigating DNA Radiation Damage Using X-Ray Absorption Spectroscopy. Biophysical Journal 110: 1304-1311 doi https://doi.org/10.1016/j.bpj.2016.01.031
D'Agata, A., Fasulo, S., Dallas, LJ., Fisher, AS., Maisano, M., Readman, JW., Jha, AN., 2014. Enhanced toxicity of 'bulk' titanium dioxide compared to 'fresh' and 'aged' nano-TiO2 in marine mussels (*Mytilus galloprovincialis*). Nanotoxicology 8: 549-558 doi 10.3109/17435390.2013.807446
Dallas, LJ., Bean, TP., Turner, A., Lyons, BP., Jha, AN., 2013. Oxidative DNA damage may not mediate Ni-induced genotoxicity in marine mussels: Assessment of genotoxic biomarkers and transcriptional responses of key stress genes. Mutation Research/Genetic Toxicology and Environmental Mutagenesis 754: 22-31 doi http://dx.doi.org/10.1016/j.mrgentox.2013.03.009
Dallas, LJ., Bean, TP., Turner, A., Lyons, BP., Jha, AN., 2016. Exposure to tritiated water at an elevated temperature: Genotoxic and transcriptomic effects in marine mussels (*M. galloprovincialis*). Journal of Environmental Radioactivity 164: 325-336 doi https://doi.org/10.1016/j.jenvrad.2016.07.034
Dallas, LJ., Keith-Roach, M., Lyons, BP., Jha, AN., 2012. Assessing the impact of ionizing radiation on aquatic invertebrates: a critical review. Radiat Res 177: 693-716
Dallas, LJ., Turner, A., Bean, TP., Lyons, BP., Jha, AN., 2018. An integrated approach to assess the impacts of zinc pyrithione at different levels of biological organization in marine mussels. Chemosphere 196: 531-539 doi https://doi.org/10.1016/j.chemosphere.2017.12.144
David, JAO., Fontanetti, CS., 2005. Surface morphology of *Mytella falcata* gill filaments from three regions of the Santos estuary. Braz J Morphol Sci 22: 203-210
Devos, A., Dallas, LJ., Voiseux, C., Lecomte-Pradines, C., Jha, AN., Fiévet, B., 2015. Assessment of growth, genotoxic responses and expression of stress related genes in the Pacific oyster *Crassostrea gigas* following chronic exposure to ionizing radiation. Marine Pollution Bulletin 95: 688-698 doi http://dx.doi.org/10.1016/j.marpolbul.2015.03.039
Dimitriadis, VK., Domouhtsidou, GP., Cajaraville, MP., 2004. Cytochemical and Histochemical Aspects of the Digestive Gland Cells of the Mussel *Mytilus galloprovincialis* (L.) in Relation to Function. Journal of Molecular Histology 35: 501-509 doi 10.1023/B:HIJO.0000045952.87268.76
DWQR., 2014. In: Millican, D. (Ed.), Drinking Water Quality Regulator for Scotland:Monitoring of Radioactivity in Scottish Drinking Water, . URL:http://dwqr.scot/media/12749/dwqr-information-letter-2014-1-monitoring-of-radioactivity-in-scottish-drinking-water.pdf, Accessed date: 07 October 2019.
Faggio, C., Tsarpali, V., Dailianis, S., 2018. Mussel digestive gland as a model tissue for assessing xenobiotics: An overview. Science of The Total Environment 636: 220-229 doi https://doi.org/10.1016/j.scitotenv.2018.04.264
Falfushynska, H., Gnatyshyna, L., Yurchak, I., Stoliar, O., Sokolova, IM., 2016. Interpopulational variability of molecular responses to ionizing radiation in freshwater bivalves *Anodonta anatina* (Unionidae). Science of The Total Environment 568: 444-456 doi https://doi.org/10.1016/j.scitotenv.2016.05.175
Farcy, E., Voiseux, C., Lebel, JM., Fievet, B., 2007. Seasonal changes in mRNA encoding for cell stress markers in the oyster *Crassostrea gigas* exposed to radioactive discharges in their natural environment. Science of The Total Environment 374: 328-341 doi http://dx.doi.org/10.1016/j.scitotenv.2006.11.014
Farcy, E., Voiseux, C., Robbes, I., Lebel, JM., Fievet, B., 2011. Effect of ionizing radiation on the transcription levels of cell stress marker genes in the Pacific oyster *Crassostrea gigas*. Radiat Res 176: 38-48
Fenech, M., Kirsch-Volders, M., Natarajan, AT., Surralles, J., Crott, JW., Parry, J., Norppa, H., Eastmond, DA., Tucker, JD., Thomas, P., 2011. Molecular mechanisms of micronucleus, nucleoplasmic bridge and nuclear bud formation in mammalian and human cells. Mutagenesis. doi 10.1093/mutage/geq052

Festarini, A., Shultz, C., Stuart, M., Kim, SB., Ferreri, C., 2015. Cellular responses to tritium exposure in rainbow trout: hto- and obt-spiked feed exposure experiments. CNL Nuclear Review 5: 155-172 doi 10.12943/CNR.2015.00059

Foster, ER., Downs, JA., 2005. Histone H2A phosphorylation in DNA double-strand break repair. FEBS Journal 272: 3231-3240 doi 10.1111/j.1742-4658.2005.04741.x

Fragkos, M., Jurvansuu, J., Beard, P., 2009. H2AX is required for cell cycle arrest via the p53/p21 pathway. Molecular and cellular biology 29: 2828-2840 doi 10.1128/mcb.01830-08

Frenzilli, G., Nigro, M., Lyons, BP., 2009. The Comet assay for the evaluation of genotoxic impact in aquatic environments. Mutation Research/Reviews in Mutation Research 681: 80-92 doi https://doi.org/10.1016/j.mrrev.2008.03.001

Gagnaire, B., Cavalie, I., Pereira, S., Floriani, M., Dubourg, N., Camilleri, V., Adam-Guillermin, C., 2015. External gamma irradiation-induced effects in early-life stages of zebrafish, *Danio rerio*. Aquat Toxicol 169: 69-78 doi 10.1016/j.aquatox.2015.10.005

Gomes, T., Song, Y., Brede, DA., Xie, L., Gutzkow, KB., Salbu, B., Tollefsen, KE., 2018. Gamma radiation induces dose-dependent oxidative stress and transcriptional alterations in the freshwater crustacean *Daphnia magna* doi 10.1016/j.scitotenv.2018.02.039

González-Romero, R., Rivera-Casas, C., Frehlick, LJ., Méndez, J., Ausió, J., Eirín-López, JM., 2012. Histone H2A (H2A.X and H2A.Z) Variants in Molluscs: Molecular Characterization and Potential Implications For Chromatin Dynamics. PLOS ONE 7: e30006 doi 10.1371/journal.pone.0030006

Graupner, A., Eide, DM., Instanes, C., Andersen, JM., Brede, DA., Dertinger, SD., Lind, OC., Brandt-Kjelsen, A., Bjerke, H., Salbu, B., Oughton, D., Brunborg, G., Olsen, AK., 2016. Gamma radiation at a human relevant low dose rate is genotoxic in mice. Scientific Reports 6: 32977 doi 10.1038/srep32977

https://www.nature.com/articles/srep32977#supplementary-information

Gómez-Mendikute, A., Elizondo, M., Venier, P., Cajaraville, MP., 2005. Characterization of mussel gill cells in vivo and in vitro. Cell and Tissue Research 321: 131-140 doi 10.1007/s00441-005-1093-9

Hagger, JAA., Franck, A., Jha, AN., 2005. Genotoxic, cytotoxic, developmental and survival effects of tritiated water in the early life stages of the marine mollusc, *Mytilus edulis*. Aquatic Toxicology 74: 205-217 doi http://dx.doi.org/10.1016/j.aquatox.2005.05.013

Han, J., Won, EJ., Lee, BY., Hwang, UK., Kim, IC., Yim, JH., Leung, KMY., Lee, YS., Lee, JS., 2014a. Gamma rays induce DNA damage and oxidative stress associated with impaired growth and reproduction in the copepod *Tigriopus japonicus*. Aquatic Toxicology 152: 264-272 doi http://dx.doi.org/10.1016/j.aquatox.2014.04.005

Han, J., Won, EJ., Kim, IC., Yim, JH., Lee, SJ., Lee, JS., 2014b. Sublethal gamma irradiation affects reproductive impairment and elevates antioxidant enzyme and DNA repair activities in the monogonont rotifer *Brachionus koreanus* doi 10.1016/j.aquatox.2014.06.009

Hartmann, A., Elhajouji, A., Kiskinis, E., Poetter, F., Martus, HJ., Fjällman, A., Frieauff, W., Suter, W., 2001. Use of the alkaline comet assay for industrial genotoxicity screening: comparative investigation with the micronucleus test. Food and Chemical Toxicology 39: 843-858 doi https://doi.org/10.1016/S0278-6915(01)00031-X

Hawkins, AJSB, B.L., 1992. Physiological interrelations, and the regulation of production. In The mussel Mytilus: ecology, physiology, genetics and culture. Amsterdam: Elsevier Science Publishers

Hoeijmakers, JHJ., 2001. Genome maintenance mechanisms for preventing cancer. Nature 411: 366-374

Hu, QH., Weng, JQ., Wang, JS., 2010. Sources of anthropogenic radionuclides in the environment: a review. Journal of Environmental Radioactivity 101: 426-437 doi https://doi.org/10.1016/j.jenvrad.2008.08.004

Hurem, S., Gomes, T., Brede, DA., Mayer, I., Lobert, VH., Mutoloki, S., Gutzkow, KB., Teien, HC., Oughton, D., Aleström, P., Lyche, JL., 2018. Gamma irradiation during gametogenesis in young adult zebrafish causes persistent genotoxicity and adverse reproductive effects. Ecotoxicology and Environmental Safety 154: 19-26 doi https://doi.org/10.1016/j.ecoenv.2018.02.031

Ivashkevich, A., Redon, CE., Nakamura, AJ., Martin, RF., Martin, OA., 2012. Use of the γ-H2AX assay to monitor DNA damage and repair in translational cancer research. Cancer Letters 327: 123-133 doi https://doi.org/10.1016/j.canlet.2011.12.025

Ivashkevich, AN., Martin, OA., Smith, AJ., Redon, CE., Bonner, WM., Martin, RF., Lobachevsky, PN., 2011. γH2AX foci as a measure of DNA damage: A computational approach to automatic analysis. Mutation Research/Fundamental and Molecular Mechanisms of Mutagenesis 711: 49-60 doi https://doi.org/10.1016/j.mrfmmm.2010.12.015

Jaeschke, BC., Bradshaw, C., 2013. Bioaccumulation of tritiated water in phytoplankton and trophic transfer of organically bound tritium to the blue mussel, *Mytilus edulis*. J Environ Radioact 115: 28-33 doi 10.1016/j.jenvrad.2012.07.008

Jaeschke, BC., Lind, OC., Bradshaw, C., Salbu, B., 2015. Retention of radioactive particles and associated effects in the filter-feeding marine mollusc *Mytilus edulis*. Science of The Total Environment 502: 1-7 doi https://doi.org/10.1016/j.scitotenv.2014.09.007

Jaeschke, BC., Millward, GE., Moody, AJ., Jha, AN., 2011. Tissue-specific incorporation and genotoxicity of different forms of tritium in the marine mussel, *Mytilus edulis*. Environmental Pollution 159: 274-280 doi http://dx.doi.org/10.1016/j.envpol.2010.08.033

Jha, AN., 2008. Ecotoxicological applications and significance of the comet assay. Mutagenesis 23: 207-221 doi 10.1093/mutage/gen014

Jha, AN., Dogra, Y., Turner, A., Millward, GE., 2005, Impact of low doses of tritium on the marine mussel, *Mytilus edulis*: Genotoxic effects and tissue-specific bioconcentration. Mutation Research/Genetic Toxicology and Environmental Mutagenesis 586: 47-57 doi http://dx.doi.org/10.1016/j.mrgentox.2005.05.008

Jha, AN., Dogra, Y., Turner, A., Millward, GE., 2006. Are low doses of tritium genotoxic to *Mytilus edulis*? Marine Environmental Research 62, Supplement 1: S297-S300 doi http://dx.doi.org/10.1016/j.marenvres.2006.04.023

Jørgensen, CB., 1982. Fluid mechanics of the mussel gill: The lateral cilia. Marine Biology 70: 275-281 doi 10.1007/BF00396846

Karatayev, AY., Boltovskoy, D., Padilla, DK., Burlakova, LE., 2007. The invasive bivalves *Dreissena polymorpha* and *Limnoperna fortunei*: parallels, contrasts, potential spread and invasion impacts. Journal of Shellfish Research 26: 205-213 doi 10.2983/0730-8000(2007)26[205:TIBDPA]2.0.CO;2

Khamis, I., Kavvadias, KC., 2012. Trends and challenges toward efficient water management in nuclear power plants. Nuclear Engineering and Design 248: 48-54 doi https://doi.org/10.1016/j.nucengdes.2012.03.039

Klobučar, GIV., Pavlica, M., Erben, R., Papeš, D., 2003. Application of the micronucleus and comet assays to mussel *Dreissena polymorpha* haemocytes for genotoxicity monitoring of freshwater environments. Aquatic Toxicology 64: 15-23 doi https://doi.org/10.1016/S0166-445X(03)00009-2

Kumaravel, TS., Jha, AN., 2006. Reliable Comet assay measurements for detecting DNA damage induced by ionising radiation and chemicals. Mutation Research/Genetic Toxicology and Environmental Mutagenesis 605: 7-16 doi http://dx.doi.org/10.1016/j.mrgentox.2006.03.002

Kumar, MKP., Shyama, SK., D'Costa, A., Kadam, SB., Sonaye, BH., Chaubey, RC., 2017. Evaluation of DNA damage induced by gamma radiation in gill and muscle tissues of

Cyprinus carpio and their relative sensitivity. Ecotoxicology and Environmental Safety 144: 166-170 doi https://doi.org/10.1016/j.ecoenv.2017.06.022

Kumar, MKP., Soorambail, KS., Bhagatsingh Harisingh, S., D'costa, A., Ramesh Chandra, C., 2015. The effect of gamma radiation on the Common carp (*Cyprinus carpio*): In vivo genotoxicity assessment with the micronucleus and comet assays. Mutation Research/Genetic Toxicology and Environmental Mutagenesis 792: 19-25 doi http://doi.org/10.1016/j.mrgentox.2015.08.005

Kuo, LJ., Yang, LX., 2008. Gamma-H2AX - a novel biomarker for DNA double-strand breaks. In vivo (Athens, Greece) 22: 305-309

Liu, M., Tee, C., Zeng, F., Sherry, JP., Dixon, B., Bols, NC., Duncker, BP., 2011. Characterization of p53 expression in rainbow trout. Comparative Biochemistry and Physiology Part C: Toxicology & Pharmacology 154: 326-332 doi https://doi.org/10.1016/j.cbpc.2011.06.018

McDonald, JH., Seed, R., Koehn, RK., 1991. Allozymes and morphometric characters of three species of *Mytilus* in the Northern and Southern Hemispheres. Marine Biology 111: 323-333 doi 10.1007/bf01319403

McDonald, P., Baxter, MS., Fowler, SW., 1993. Distribution of radionuclides in mussels, winkles and prawns. Part 2. Study of organisms under laboratory conditions using alpha-autoradiography. Journal of Environmental Radioactivity 18: 203-228 doi http://dx.doi.org/10.1016/0265-931X(93)90028-6

Mersch, J., Beauvais, MN., Nagel, P., 1996. Induction of micronuclei in haemocytes and gill cells of zebra mussels, *Dreissena polymorpha*, exposed to clastogens. Mutat Res 371: 47-55

Nalepa, TF., Gardner, WS., Malczyk, JM., 1991. Phosphorus cycling by mussels (Unionidae : Bivalvia) in Lake St. Clair. Hydrobiologia 219: 239-250

Nalepa, TF., Schloesser, DW., 1992. Zebra mussels biology, impacts, and control. CRC Press

NOAA., 2012. Pollution :Changes Over Time: How NOAA's Mussel Watch Program is Adapting to the Needs of Coastal Communities. In: Lauenstein G (ed)

Oommen, D., Dodd, NJF., Yiannakis, D., Moyeed, R., Jha, AN., 2016a. Linking genotoxicity and cytotoxicity with membrane fluidity: A comparative study in ovarian cancer cell lines following exposure to auranofin. Mutation Research/Genetic Toxicology and Environmental Mutagenesis 809: 43-49 doi https://doi.org/10.1016/j.mrgentox.2016.09.003

Oommen, D., Yiannakis, D., Jha, AN., 2016b. BRCA1 deficiency increases the sensitivity of ovarian cancer cells to auranofin. Mutation Research/Fundamental and Molecular Mechanisms of Mutagenesis 784-785: 8-15 doi https://doi.org/10.1016/j.mrfmmm.2015.11.002

Parolini, M., Quinn, B., Binelli, A., Provini, A., 2011. Cytotoxicity assessment of four pharmaceutical compounds on the zebra mussel (*Dreissena polymorpha*) haemocytes, gill and digestive gland primary cell cultures. Chemosphere 84: 91-100 doi https://doi.org/10.1016/j.chemosphere.2011.02.049

Pearson, HBC., Dallas, LJ., Comber, SDW., Braungardt, CB., Worsfold, PJ., Jha, AN., 2018. Mixtures of tritiated water, zinc and dissolved organic carbon: Assessing interactive bioaccumulation and genotoxic effects in marine mussels, *Mytilus galloprovincialis*. Journal of Environmental Radioactivity 187: 133-143 doi https://doi.org/10.1016/j.jenvrad.2017.12.018

Pereira, S., Bourrachot, S., Cavalie, I., Plaire, D., Dutilleul, M., Gilbin, R., Adam-Guillermin, C., 2011. Genotoxicity of acute and chronic gamma-irradiation on zebrafish cells and consequences for embryo development. Environ Toxicol Chem 30: 2831-2837 doi 10.1002/etc.695

Pereira, S., Malard, V., Ravanat, JL., Davin, AH., Armengaud, J., Foray, N., Adam-Guillermin, C., 2014. Low Doses of Gamma-Irradiation Induce an Early Bystander Effect in Zebrafish Cells Which Is Sufficient to Radioprotect Cells. PLoS ONE 9: e92974 doi 10.1371/journal.pone.0092974

Podhorecka, M., Skladanowski, A., Bozko, P., 2010. H2AX Phosphorylation: Its Role in DNA Damage Response and Cancer Therapy. Journal of Nucleic Acids 2010: 9 doi 10.4061/2010/920161

Ramakers, C., Ruijter, JM., Deprez, RH., Moorman, AF., 2003. Assumption-free analysis of quantitative real-time polymerase chain reaction (PCR) data. Neurosci Lett 339: 62-66

Redon, CE., Dickey, JS., Bonner, WM., Sedelnikova, OA., 2009. γ-H2AX as a biomarker of DNA damage induced by ionizing radiation in human peripheral blood lymphocytes and artificial skin. Advances in Space Research 43: 1171-1178 doi https://doi.org/10.1016/j.asr.2008.10.011

Revet, I., Feeney, L., Bruguera, S., Wilson, W., Dong, TK., Oh, DH., Dankort, D., Cleaver, JE., 2011. Functional relevance of the histone γH2Ax in the response to DNA damaging agents. Proceedings of the National Academy of Sciences 108: 8663

Rhee, JS., Kim, BM., Kang, CM., Lee, YM., Lee, JS., 2012. Gamma irradiation-induced oxidative stress and developmental impairment in the hermaphroditic fish, *Kryptolebias marmoratus* embryo. Environ Toxicol Chem 31: 1745-1753 doi 10.1002/etc.1873

Ruijter, JM., Ramakers, C., Hoogaars, WM., Karlen, Y., Bakker, O., van den Hoff, MJ., Moorman, AF., 2009. Amplification efficiency: linking baseline and bias in the analysis of quantitative PCR data. Nucleic Acids Res 37: e45 doi 10.1093/nar/gkp045

Salbu, B., Kashparov, V., Lind, OC., Garcia-Tenorio, R., Johansen, MP., Child, DP., Roos, P., Sancho, C., 2018. Challenges associated with the behaviour of radioactive particles in the environment. Journal of Environmental Radioactivity 186: 101-115 doi https://doi.org/10.1016/j.jenvrad.2017.09.001

Sancar, LALB., Ünsal-Kaçmaz, K., Linn, S., 2004. Molecular Mechanisms of Mammalian DNA Repair and the DNA Damage Checkpoints. Annual Review of Biochemistry 73: 39-85 doi doi:10.1146/annurev.biochem.73.011303.073723

Sarkar, A., Bhagat, J., Ingole, BS., Rao, DP., Markad, VL., 2015. Genotoxicity of cadmium chloride in the marine gastropod *Nerita chamaeleon* using comet assay and alkaline unwinding assay. Environ Toxicol 30: 177-187 doi 10.1002/tox.21883

Sastry, AN., Blake, NJ., 1971. Regulation of gonad development in the bay scallop, *Aequipecten irradians* lamarck. The Biological Bulletin 140: 274-283 doi 10.2307/1540074

Sayed, AEDH., Igarashi, K., Watanabe-Asaka, T., Mitani, H., 2017. Double strand break repair and γ-H2AX formation in erythrocytes of medaka (*Oryzias latipes*) after γ-irradiation. Environmental Pollution 224: 35-43 doi https://doi.org/10.1016/j.envpol.2016.11.050

Schnug, L., Jensen, J., Scott-Fordsmand, JJ., Leinaas, HP., 2014. Toxicity of three biocides to springtails and earthworms in a soil multi-species (SMS) test system. Soil Biology and Biochemistry 74: 115-126 doi https://doi.org/10.1016/j.soilbio.2014.03.007

Scoppa, P., 1983. Accumulation of radionuclides in aquatic organisms. Inorganica Chimica Acta 79: 231 doi https://doi.org/10.1016/S0020-1693(00)95270-8

Sedelnikova, OA., Pilch, DR., Redon, C., Bonner, WM., 2003. Histone H2AX in DNA damage and repair. Cancer Biology and Therapy. 2:3, pp 233-235

SEPA., 2013. Phosphorus-32 Concentrations in the River Clyde, Scotland between 2005-2013. Scottish Environmental Protection Agency. Personal communication.

Sforzini, S., Oliveri, C., Orrù, A., Chessa, G., Pacchioni, B., Millino, C., Jha, AN., Viarengo, A., Banni, M., 2018. Application of a new targeted low density microarray and conventional biomarkers to evaluate the health status of marine mussels: A field study in Sardinian coast, Italy. The Science of the total environment 628-629: 319-328 doi 10.1016/j.scitotenv.2018.01.293

Skipperud, L., Salbu, B., 2018. Radionuclides: Sources, Speciation, Transfer and Impacts in the Aquatic and Terrestrial Environment. In: Dellasala DA, Goldstein MI (eds) Encyclopedia of the Anthropocene. Elsevier, Oxford, pp 195-206

Smith, JT., Bowes, MJ., Cailes, CR., 2011. A review and model assessment of (32)P and (33)P uptake to biota in freshwater systems. J Environ Radioact 102: 317-325 doi 10.1016/j.jenvrad.2010.12.006

Solomon, KR., Sibley, P., 2002. New concepts in ecological risk assessment: where do we go from here? Marine Pollution Bulletin 44: 279-285 doi https://doi.org/10.1016/S0025-326X(01)00252-1

Souza, DS., Ramos, AP., Nunes, FF., Moresco, V., Taniguchi, S., Leal, DA., Sasaki, ST., Bicego, MC., Montone, RC., Durigan, M., Teixeira, AL., Pilotto, MR., Delfino, N., Franco, RM., Melo, CM., Bainy, AC., Barardi, CR., 2012. Evaluation of tropical water sources and mollusks in southern Brazil using microbiological, biochemical, and chemical parameters. Ecotoxicol Environ Saf 76: 153-161 doi 10.1016/j.ecoenv.2011.09.018

Strober, W., 2001. Trypan blue exclusion test of cell viability. Curr Protoc Immunol Appendix 3: Appendix 3B doi 10.1002/0471142735.ima03bs21

UNSCEAR., 1982. Ionizing radiation: sources and biological effects. United Nations Scientific Committee on the Effects of Atomic Radiation

Venier, P., Maron, S., Canova, S., 1997. Detection of micronuclei in gill cells and haemocytes of mussels exposed to benzo[a]pyrene. Mutation Research/Genetic Toxicology and Environmental Mutagenesis 390: 33-44 doi https://doi.org/10.1016/S0165-1218(96)00162-0

Vernon, EL., Smith, JT., Jha, AN., 2018. Relative comparison of tissue specific bioaccumulation and radiation dose estimation in marine and freshwater bivalve molluscs following exposure to phosphorus-32. Journal of Environmental Radioactivity 192: 312-320 doi https://doi.org/10.1016/j.jenvrad.2018.07.005

Vernon, EL., Jha, AN., 2019. Assessing relative sensitivity of marine and freshwater bivalves following exposure to copper: Application of classical and novel genotoxicological biomarkers. Mutation Research/Genetic Toxicology and Environmental Mutagenesis. 842: 60-71
doi 10.1016/j.mrgentox.2019.01.008

Viarengo, A., Lowe, D., Bolognesi, C., Fabbri, E., Koehler, A., 2007. The use of biomarkers in biomonitoring: A 2-tier approach assessing the level of pollutant-induced stress syndrome in sentinel organisms. Comparative Biochemistry and Physiology Part C: Toxicology & Pharmacology 146: 281-300 doi https://doi.org/10.1016/j.cbpc.2007.04.011

Vincent-Hubert, F., Arini, A., Gourlay-Francé, C., 2011. Early genotoxic effects in gill cells and haemocytes of *Dreissena polymorpha* exposed to cadmium, B[a]P and a combination of B[a]P and Cd. Mutation Research/Genetic Toxicology and Environmental Mutagenesis 723: 26-35 doi http://dx.doi.org/10.1016/j.mrgentox.2011.03.008

Figure and Table Captions

Figure 1. Schematic diagram showing experimental design. Images from *M. galloprovincialis* digestive gland cells.

Figure 2. Genotoxic effects in *M. galloprovincialis* and *D. polymorpha* gill cells following a 10-day exposure to ^{32}P. Asterisks (*, ** or ***) are indicative of significant differences (p < 0.05, 0.01, 0.001) from the corresponding control. SD is standard deviation of mean data. n=9.

Figure 3. Pearson's correlation analyses of: (top to bottom) % tail DNA and induction of MN, % tail DNA and γ-H2AX foci, and induction of MN and γ-H2AX foci. *M. galloprovincialis* digestive gland (left) and *M. galloprovincialis* gill (right). n=9.

Figure 4. Pearson's correlation analyses of: (top to bottom) % tail DNA and induction of MN, % tail DNA and γ-H2AX foci, and induction of MN and γ-H2AX foci. *D. polymorpha* digestive gland (left) and *D. polymorpha* gill (right). n=9.

Figure 5. Relative expression ratios (RER) of key genes in *M. galloprovincialis* and *D. polymorpha* gill and digestive gland cells following a 10-day exposure to ^{32}P. Data are normalised for reference genes (*ef1, actin*) and controls. Error bars indicate the 95% confidence intervals. Asterisks (*, ** or ***) are indicative of significant differences (p < 0.05, 0.01, 0.001) from the corresponding control. n=9.

Table 1. Water quality parameters (pH, temperature, salinity and dissolved oxygen [DO]), copper concentrations in water (µg L^{-1}) and ^{32}P concentrations in water (Bq L^{-1}), for both species. Data is presented as mean ± standard deviation.

Table 2. Gene and primers used for *M. galloprovincialis* and *D. polymorpha* in RT-PCR.

Table 3. Table to show (a) the expected dose rates in mGy d^{-1} and (b) the average dose rate achieved in *M. galloprovincialis* and *D. polymorpha* whole-body, digestive gland and gill tissue (mGy d^{-1}). Values in bold are those above the ERICA tool screening value of 0.24 mGy d^{-1}.